A Cas-BCAR3 co-regulatory circuit controls lamellipodia dynamics

Elizabeth M. Steenkiste[1,2], Jason D. Berndt[1,3]*, Carissa Pilling[1]*, Christopher Simpkins[1] and Jonathan A. Cooper[1,2]

[1] Division of Basic Sciences, Fred Hutchinson Cancer Research Center, 1100 Fairview Avenue N, Seattle Washington 98109

[2] Molecular and Cellular Biology Program, University of Washington, Seattle, Washington 98195

[3] Present address: PreCyte Inc, Seattle Washington 98109

* Equal contributions

Corresponding author:

Jonathan A. Cooper

office: 206-667-4454

cell: 206-604-6206

email: jcooper@fredhutch.org

Abstract

Cell migration involves positive and negative feedback loops that coordinate integrin engagement with lamellipodial protrusion. A key player is Cas (p130Cas, BCAR1), whose integrin-induced phosphorylation stimulates actin polymerization at the cell edge and formation of a ruffling lamellipodium. Cas phosphorylation also stimulates Cas downregulation by the ubiquitin-proteasome pathway, ensuring negative feedback. Although Cas appears to be mechanosensitive, it remains unclear how integrins stimulate Cas phosphorylation. Cas associates with integrin adhesions through its N and C termini. The C terminus of Cas binds to an SH2 domain protein, BCAR3, but the importance of this interaction is unclear. Here, we find that, like Cas, BCAR3 is also activated by phosphorylation and inactivated by the ubiquitin-proteasome system. BCAR3 is necessary for Cas phosphorylation but not Cas localization. Instead, BCAR3 requires Cas for localization. We identify a single phosphorylation site in BCAR3 that is required for both Cas activation and for BCAR3 turnover. Mutation of this site inhibits BCAR3 turnover, Cas phosphorylation, lamellipodium ruffling and migration. This places BCAR3 in a co-regulatory positive-feedback circuit with Cas, with BCAR3 requiring Cas for localization and Cas requiring BCAR3 for activation. The use of a single phosphorylation site in BCAR3 for activation and degradation ensures reliable negative feedback by the ubiquitin-proteasome system.

Introduction

Cell migration requires accurate spatial and temporal coordination of actin polymerization, cell-cell and cell-matrix adhesions, microtubules, actomyosin contraction, vesicle traffic, and membrane composition. Breakdown of coordination leads to pathologies in morphogenesis, wound healing and cancer (Trepat et al., 2012). At the front of the cell, formation of nascent adhesion complexes activates branched actin polymerization to form a thin, dynamic lamellipodium (Bachir et al., 2017, Legate et al., 2009). Actin polymerization creates a rearward flow of actin that interacts with exposed actin-binding sites on integrin-associated talin and vinculin, forming catch bonds and clustering the integrins into focal complexes (FCs) (Case et al., 2015, Galbraith et al., 2002, Partridge et al., 2006). Most FCs are short-lived, but some mature into focal adhesions (FAs) at the base of the lamellipodium, anchoring actin stress fibers and providing resistance to actomyosin contractile forces (del Rio et al., 2009, Puklin-Faucher et al., 2009, Tadokoro et al., 2003). Integrin adhesions are also sources of biochemical signals, where multiple proteins are phosphorylated by focal adhesion kinase (FAK) and Src-family kinases (SFKs) (Burridge et al., 1992, Huang et al., 1993, Miyamoto et al., 1995, Schaller et al., 1992). Some integrin-stimulated phosphorylation events regulate protein-protein interactions within the adhesion (Pasapera et al., 2010, Stutchbury et al., 2017, Zaidel-Bar et al., 2007), while others activate signaling proteins that coordinate adhesion with lamellipodium dynamics and other aspects of cell biology, such as cell survival (Mitra et al., 2006). One important adhesion-regulated signaling protein is Cas (Crk-associated substrate, also called p130Cas or BCAR1), which plays a critical role in lamellipodium protrusion, membrane ruffling, adhesion assembly, adhesion turnover, resistance to anoikis and malignant transformation (Honda et al., 1999, Sanders et al., 2005, Sharma et al., 2008, Webb et al., 2004) (reviews (Defilippi et al., 2006, Tikhmyanova et al., 2010)).

Cas activation involves phosphorylation at multiple YxxP sites in a predicted unstructured region near the N terminus, known as the “substrate domain” (see Figure 1a for a diagram of Cas structure). Phosphorylation at these sites recruits adaptor proteins Crk and CrkL and their associated guanine nucleotide exchange factors (GEFs), C3G for Rap1 and DOCK1 (also called DOCK180) for Rac1 (Fonseca et al., 2004, Goldberg et al., 2003, Hasegawa et al., 1996, Kiyokawa et al., 1998, Klemke et al., 1998, Sakai et al., 1994, Sakai et al., 1997, Tanaka et al., 1994). Active Rap1 increases talin recruitment to integrins to promote adhesion maturation (Boettner et al., 2009), while Rac1 stimulates polymerization of branched actin structures by WAVE, leading to lamellipodial protrusion and ruffling (Cheresh et al., 1999, DeMali et al., 2002,

Ridley 2001, Ridley et al., 1992, Stradal et al., 2004). Thus, Cas is part of a self-reinforcing cycle in which actin polymerization stimulates Cas phosphorylation, which leads to more actin polymerization, lamellipodium protrusion and membrane ruffling. Cas also stimulates migration by increasing focal adhesion turnover as the cell move forwards (Ren et al., 2000, Rottner et al., 1999, Webb et al., 2004).

Cas is also subject to negative feedback. Phosphorylation of a YDYV sequence, C-terminal to the substrate domain (Figure 1a), mediates turnover of pY-Cas. This phosphosite binds to the SH2 domain of SOCS6 (suppressor of cytokine signaling 6), recruiting CRL5 (Cullin 5-RING-ligase) and targeting Cas to the ubiquitin-proteasome system (Teckchandani et al., 2014). SOCS6 co-localizes with phosphorylated Cas in adhesions at the leading edge of migrating cells where it suppresses adhesion dynamics (Teckchandani et al., 2016). Mutation of the YDYV sequence or knockdown of SOCS6 or Cullin 5 (Cul5) stabilizes Cas and increases lamellipodia protrusion and ruffling (Teckchandani et al., 2014). Thus, phosphorylation provides negative feedback onto Cas, restraining leading edge dynamics and stabilizing adhesions.

While the effects of Cas YxxP phosphorylation are well understood, it is less clear how Cas phosphorylation is regulated. Phosphorylation is stimulated by integrin-dependent actin polymerization at the leading edge and requires an intact actin cytoskeleton (Vuori et al., 1996, Vuori et al., 1995, Zhang et al., 2014, Zhao et al., 2016). The substrate domain is more accessible for phosphorylation when it is extended (Hotta et al., 2014, Sawada et al., 2006, Tamada et al., 2004). One idea is that the substrate domain is extended by forces acting on proteins bound to the N- and C-terminal Src homology 3 (SH3) and Cas C-terminal homology (CCH)/focal adhesion targeting (FAT) domains (Figure 1a). Both domains are required to localize Cas to integrin adhesions (Branis et al., 2017, Donato et al., 2010, Harte et al., 1996, Nakamoto et al., 1997, Nojima et al., 1995, Vuori et al., 1995). The Cas SH3 binds adhesion proteins vinculin and FAK, either of which could localize Cas to adhesions and exert force (Harte et al., 1996, Janostiak et al., 2014, Polte et al., 1995). In addition, Cas binds N-WASP through FAK, and N-WASP stimulates actin polymerization at the membrane during cell spreading (Kostic et al., 2006, Wu et al., 2004, Zhang et al., 2014). However, the role of the Cas CCH/FAT domain is less clear. It binds to LIM domain proteins paxillin, zyxin and ajuba, and to a CDC25 homology (CDC25H) domain found in NSP family proteins (Mace et al., 2011, Pratt et al., 2005, Wallez et al., 2012, Yi et al., 2002, Zhang et al., 2017) (Figure 1a). It is unclear which, if any, of these proteins is responsible for localizing the Cas CCH/FAT domain to adhesions.

The NSP proteins, comprised of BCAR3 (breast cancer anti-estrogen resistance 3, also called AND-34, NSP2, Sh2d3b), NSP1 (Sh2d3a) and NSP3 (Shep1, Chat, Sh2d3c), are defined by a common structure with an SH2 domain and CDC25H domain (Figure 1a). NSP proteins cooperate with Cas-family proteins in cell migration (Wallez et al., 2012). For example, over-expressed BCAR3 increases Cas phosphorylation, Cas localization to membrane ruffles, cell migration, cell proliferation, and, like Cas, protects estrogen-dependent breast cancer cells from inhibitory actions of anti-estrogens (Cai et al., 2003, Cross et al., 2016, Riggins et al., 2003, Roselli et al., 2010, Schrecengost et al., 2007, Schuh et al., 2010, van Agthoven et al., 1998). BCAR3 regulates EGF- and insulin-stimulated membrane ruffling (Oh et al., 2013, Schrecengost et al., 2007). BCAR3 is phosphorylated at unidentified tyrosine residues in response to serum and adhesion (Cai et al., 1999) and the SH2 domain can bind the epidermal growth factor (EGF) receptor (Oh et al., 2008). In mouse fibroblasts, the BCAR3 SH2-domain binds phosphorylated PTPRA (RPTPα), a protein phosphatase that activates SFKs and is required to localize BCAR3 to the cell edge and activate Cas (Sun et al., 2012, von Wichert et al., 2003, Zheng et al., 2000). These studies show that BCAR3 is intimately involved in Cas regulation, but leave open questions of how BCAR3 itself is regulated and how it regulates Cas.

Here, using normal epithelial cells, we find that BCAR3, like Cas, is subject to negative regulation by the ubiquitin-proteasome system. BCAR3 phosphorylation at Y117 recruits SOCS6 and leads to Cul5-dependent degradation. BCAR3 is needed for cell migration and invasion, and for increased lamellipodial ruffling and collective migration when Cul5 is absent. Using gene silencing and mutant analysis, we find that BCAR3 localization to adhesions requires the Cas-binding site but not Y117 or the SH2 domain. Reciprocally, Cas phosphorylation requires BCAR3's Y117, SH2 domain and Cas-binding site. BCAR3 and Cas thus form a signaling hub that localizes to active integrins and coordinates actin dynamics under negative control by the ubiquitin proteasome system.

Results

CRL5 regulates BCAR3 protein turnover

We previously reported that CRL5 inhibits Src activity and Src-dependent transformation of MCF10A epithelial cells, in part by targeting pY proteins such as pYCas for degradation by the ubiquitin-proteasome system (Teckchandani et al., 2014). Because overexpression of Cas does not increase migration (Teckchandani et al., 2014), we infer that CRL5 may target additional phosphoproteins that, with Cas, are required for increased migration. We sought to identify such phosphoproteins by screening for pY peptides whose abundance increases when Cul5 is inhibited. To this end, control and Cul5-deficient MCF10A cells were lysed under denaturing conditions, proteins were digested with trypsin, and peptides were labeled with isobaric TMT tags for quantitative pY proteomics (Zhang et al., 2007). In one experiment, samples were prepared from control and Cul5-deficient cells that were starved for epidermal growth factor (EGF) for 0, 24 or 72 hr. Starvation time had no systematic effect on peptide abundance, so, in a second experiment, we prepared biological triplicate samples from growing control and Cul5-deficient cells. Sixteen pY peptides increased significantly in Cul5-deficient cells in both experiments, including pY128 from Cas and pY117 and pY266 from BCAR3 (Figure 1b, Figure 1 – Figure Supplement 1). We decided to focus on BCAR3 because Cul5 regulates Cas and Cas binds BCAR3 (Wallez et al., 2012).

The increased quantity of BCAR3 pY peptides in Cul5-deficient cells could result from increased phosphorylation, increased protein level, or both. We used immunoblotting to test whether BCAR3 protein level is regulated by Cul5. BCAR3 protein level increased approximately 4-fold in Cul5-deficient cells, in either growth or starvation conditions (Figure 1c). However, RNA levels were unaltered (Figure 1c), consistent with altered protein synthesis or degradation. To measure degradation, we inhibited new protein synthesis with cycloheximide and monitored BCAR3 protein level. BCAR3 half-life was approximately 4 hours in control cells but greater than 8 hours in Cul5-deficient cells (Figure 1d). BCAR3 degradation was inhibited by Cullin neddylation inhibitor MLN4924 or proteasome inhibitor MG132, but not by lysosome inhibitor Bafilomycin (Fig 1e). These results suggest that CRL5 regulates BCAR3 turnover by the ubiquitin-proteasome system and that the increase in BCAR3 pY117 and pY266 in Cul5-deficient cells is likely due to an increased availability of BCAR3 protein for phosphorylation rather than, or in addition to, an increase in kinase activity.

BCAR3 regulates epithelial cell migration

BCAR3 is required for the migration of cancer cells and fibroblasts (Cross et al., 2016, Schrecengost et al., 2007, Sun et al., 2012) but its importance in normal epithelial cells is unknown. BCAR3 loss of function induced by siRNA transfection or *BCAR3* gene disruption in MCF10A cells slowed migration and invasion toward a source of the chemoattractant EGF in modified Boyden chamber assays (Figure 2a-c, Figure 2 - Figure Supplement 1). BCAR3 was required for migration and invasion of both normal and Cul5-deficient cells, suggesting the existence of multiple pathways acting in parallel to control single-cell migration. In contrast, in scratch wound assays without added EGF, loss of BCAR3 slowed migration in Cul5-deficient cells but had little effect in normal cells, suggesting that Cul5 inhibits collective-cell migration through BCAR3 (Figure 2d). Inspection of the wound edge revealed that BCAR3 is also needed for the increased lamellipodia length and ruffling in Cul5-depleted cells (Figure 2e-g). This epistatic relationship is consistent with CRL5 inhibiting BCAR3-dependent collective-cell migration and lamellipodia dynamics. EGF may overcome this regulation in single-cell migration assays by stimulating parallel pathways.

CRL5 separately targets BCAR3 and Cas through SOCS6

CRL5 promotes ubiquitination and degradation of substrate proteins bound to adaptor proteins (Okumura et al., 2016). CRL5 adaptors include SOCS family proteins, which contain SH2 domains for binding to pY. To test whether SOCS proteins bind BCAR3, we transiently expressed T7-tagged SOCS proteins and assayed binding to endogenous BCAR3 by immunoprecipitation and immunoblotting. BCAR3 specifically co-precipitated with SOCS6, the same adaptor that binds Cas (Figure 3a) (Teckchandani et al., 2014). Accordingly, SOCS6 loss of function in MCF10A cells increased BCAR3 steady-state protein levels and decreased the rate of BCAR3 turnover (Figure 3b,c). Together, these results suggest that $CRL5^{SOCS6}$ mediates BCAR3 turnover.

Since BCAR3 and Cas bind each other and both are bound and regulated by SOCS6, it is possible that SOCS6 binds BCAR3 indirectly, through Cas. We tested this possibility by two strategies (Figure 3d). First, we used a BCAR3 mutant, L744E/R748E, called here $BCAR3^{EE}$, that does not bind Cas (Wallez et al., 2014). This mutation inhibited binding to Cas but not SOCS6 (Figure 3e). Second, we found that BCAR3-SOCS6 binding occurred in cells from which Cas had been depleted with siRNA (Figure 3f). Collectively, these data suggest that SOCS6 binds BCAR3 and Cas independently.

CRL5 binds BCAR3 pY117

We considered that SOCS6 might bind BCAR3 through pY-dependent or -independent interactions. A cell-permeable phosphotyrosine phosphatase inhibitor, pervanadate, increased BCAR3-SOCS6 association, suggesting pY dependence (Figure 4a). In addition, disrupting the SOCS6 SH2 domain by deletion (ΔC) or point mutation (R407K) inhibited binding to BCAR3 (Figure 4b). This suggests that the SOCS6 SH2 domain binds pY-BCAR3. Serum or adhesion stimulates tyrosine phosphorylation of BCAR3 in mouse fibroblasts (Cai et al., 1999), but the specific sites have not been identified. High-throughput pY proteomics surveys have identified phosphorylation of BCAR3 at tyrosine residues 42, 117, 212, 266 and 429 in over 25 mouse and human cell lines (Hornbeck et al., 2019). We tested whether these sites were required for binding SOCS6 using site-directed mutagenesis (Figure 4c). An F5 mutant, in which all five tyrosines were changed to phenylalanine, was unable to bind SOCS6 (Figure 4d). By mutating each pY site individually we found that Y117 is necessary to bind SOCS6 (Figure 4d). Furthermore, mutating all sites except Y117 (42, 212, 266 and 429) had little effect on SOCS6 binding (BCAR3 4F mutant, Figure 4e). These results support a model in which phosphorylation of BCAR3 at Y117 is both necessary and sufficient to bind the SOCS6 SH2 domain.

Y117 and Cas regulate BCAR3 protein stability

To test whether Y117 is required for CRL5-dependent BCAR3 protein turnover in cells, we measured the effect of Y117F mutation on the level of tagged BCAR3 protein in control and Cul5-deficient cells. To avoid possible artifacts due to over-expression, we used a doxycycline inducible promoter (Baron et al., 1997). MCF10A cells were first transduced to express the reverse *tet* transactivator (rtTA), and then transduced to express tagged wildtype or mutant BCAR3 under control of the *tet* operator. BCAR3 was tagged at the N-terminus with a V5 epitope for immunoblotting and a SNAP domain (O^6-alkylguanine-DNA alkyltransferase) that allows covalent labelling with benzyl guanine compounds (Keppler et al., 2003). Stably selected cell lines were treated with doxycycline (dox) to induce protein expression and with various siRNAs to regulate expression of endogenous BCAR3 or Cul5. Initial characterization showed that 10 ng/mL dox induced expression of wildtype SNAP-V5-BCAR3 to approximately the same level as endogenous BCAR3, while SNAP-V5-BCAR3^{Y117F} was expressed at approximately two-fold higher level (Figure 5a). Notably, Cul5 depletion increased the level of SNAP-V5-BCAR3^{WT} more than 2-fold while the level of SNAP-V5-BCAR3^{Y117F} was unchanged (Fig 5b). These results suggest that phosphorylation at Y117 is required for Cul5-dependent BCAR3 protein turnover in cells, consistent with SOCS6 binding to this site.

We extended this approach to test the importance of the BCAR3 SH2 domain and the Cas-binding site for Cul5-dependent turnover. To inactivate the BCAR3 SH2 domain, we created an arginine to lysine at residue 177 (R177K), which lies in the consensus FLVRES motif and is required to bind the pY phosphate (Jaber Chehayeb et al., 2020, Marengere et al., 1994). To inhibit Cas binding, we used the aforementioned L744E/R748E mutant (BCAR3^{EE}). Cul5-depletion increased the level of SNAP-V5-BCAR3^{R177K} but not SNAP-V5-BCAR3^{EE} (Figure 5c). Taken together, the results suggest that CRL5^{SOCS6} regulates BCAR3 protein turnover dependent on Cas binding and on Y117 phosphorylation. The BCAR3 SH2 domain is dispensable for degradation, and, by implication, may not be needed for Y117 phosphorylation.

Lamellipodial ruffling and cell migration require BCAR3 Y117, SH2 domain and Cas binding

Since BCAR3^{Y117F} accumulates to higher levels in cells, we suspected it may be more active in biological assays. Over-expression of BCAR3 in fibroblasts and breast cancer cells stimulates Cas-dependent functions, such as lamellipodia ruffling (Cai et al., 2003, Wallez et al., 2014, Wilson et al., 2013). Similarly, induction of SNAP-V5-BCAR3^{WT} increased membrane ruffling in MCF10A cells (Figure 6a). In contrast, over-expressed SNAP-V5-BCAR3^{Y117F} did not increase ruffling (Figure 6a). SNAP-V5-BCAR3^{R177K} and SNAP-V5-BCAR3^{EE} were also inactive. This suggests that not only is Y117 needed for downregulation of BCAR3 by CRL5^{SOCS6}, it is also needed, together with the SH2 domain and Cas binding, for over-expressed BCAR3 to increase lamellipodial ruffling.

While BCAR3 over-expression was not sufficient to increase migration (Figure 6 - Figure Supplement 1), BCAR3 was necessary for the increased migration and ruffling of Cul5-deficient cells (Figure 2). To test which domains of BCAR3 are necessary, we knocked down Cul5 and endogenous BCAR3 and induced wildtype or mutant SNAP-V5-BCAR3 at endogenous level. While wildtype SNAP-V5-BCAR3 rescued the increased migration and ruffling of Cul5-deficient cells, none of the mutants, Y117F, R177K or EE, were active (Figure 6b). Thus, all three of these regions of BCAR3 regulate lamellipodial dynamics and cell migration when Cul5 is absent.

Cas recruits BCAR3 to integrin adhesions, where BCAR3 stimulates Cas phosphorylation, dependent on BCAR3 Y117 and SH2

These findings raise the question of how BCAR3 Y117, SH2 domain and Cas binding cooperate to regulate membrane ruffling and migration. One possibility is that BCAR3 is important to localize Cas, as suggested by others (Makkinje et al., 2009, Schrecengost et al., 2007, Sun et al., 2012). Cas could then activate lamellipodia dynamics through the Crk/DOCK180/Rac pathway (Klemke et al., 1998, Sakai et al., 1994, Sanders et al., 2005, Sharma et al., 2008). In that case, BCAR3's Y117, SH2 domain and/or Cas-binding site may be needed for Cas localization. Alternatively, BCAR3 may regulate Cas activation but not localization. To explore these possibilities, we monitored the effect of BCAR3 depletion on the localization of YFP-Cas and the effect of Cas depletion on the localization of SNAP-V5-BCAR3^{WT}. Localization was quantified in leading edge adhesions relative to the adhesion marker paxillin. We found that YFP-Cas localized properly to adhesions in control and BCAR3-depleted cells (Figure 7a). In contrast, SNAP-V5-BCAR3^{WT} localization was disrupted when Cas was depleted (Figure 7b). Thus, BCAR3 requires Cas to localize to adhesions, rather than vice versa. Consistent with this interpretation, Cas-binding mutant SNAP-V5-BCAR3^{EE} did not localize to leading edge adhesions, while SNAP-V5-BCAR3^{Y117F} and BCAR3^{R177K}, which have the ability to bind Cas (Figure 8- Figure Supplement 1), localized normally (Figure 8a, b). Therefore, it is likely that defects in Cas activation rather than reduced Cas recruitment to adhesions explain the inability of SNAP-V5-BCAR3^{EE} and other mutants to promote membrane ruffling and migration.

To assay Cas activation in adhesions, we used antibodies to pY165, one of the repeated YxxP motifs in Cas that are required for binding to Crk (Fonseca et al., 2004, Sakai et al., 1994, Songyang et al., 1993). As expected, SNAP-V5-BCAR3^{WT} rescued Cas phosphorylation in BCAR3-depleted cells (Figure 8a, c). However, Cas was not phosphorylated in cells expressing Y117F, R177K or EE mutants of SNAP-V5-BCAR3 (Figure 8a, c). This suggests that BCAR3 not only has to be bound to Cas but also needs to be phosphorylated at Y117 and to interact with proteins through its SH2 domain in order for Cas phosphorylation to occur. The phosphorylation of Cas in adhesions correlates with the rescue of ruffling (Figures 6b and 8). Taken together, these results suggest that BCAR3 is brought to integrin adhesions by binding to Cas, then uses its pY117 and SH2 domain to activate Cas phosphorylation and downstream signaling, leading to lamellipodial ruffling.

Discussion

Cell migration requires biophysical and biochemical signaling between the leading edge and adhesion complexes, so that adhesion assembly and disassembly is coordinated with actin polymerization, anchorage of stress fibers and generation of traction forces (Trepat et al., 2012). Our results address one aspect of this complicated process: the linkage between integrin engagement and lamellipodial extension. Previous studies have found that Cas and BCAR3 synergize for lamellipodium ruffing and cell migration, but they also cross-regulate protein expression, so the mechanism has been unclear (Cai et al., 1999, Cross et al., 2016, Riggins et al., 2003, Schrecengost et al., 2007, Wallez et al., 2014). Here, using loss-of-function approaches, we find that there is positive feedback between Cas and BCAR3, and dual negative feedback on both proteins by the ubiquitin-proteasome system.

Our results support a multi-step model (Figure 8 – figure supplement 2). First, Cas is recruited to active integrins near the leading edge of migrating cells. Cas recruitment does not require BCAR3, but BCAR3 recruitment does require Cas. Since most BCAR3 in the cell is complexed with Cas (Cross et al., 2016), the two proteins are likely recruited jointly, via localization signals on Cas. We do not know where or how BCAR3 Y117 is phosphorylated, but infer it requires Cas association because the Cas-binding mutant is not regulated by Cul5. Once bound, BCAR3 stimulates Cas phosphorylation on its YxxP motifs in a mechanism that requires the BCAR3 SH2 domain and pY117. Cas phosphorylation then drives membrane ruffling by well-documented mechanisms involving Crk, DOCK180 and Rac (Cheresh et al., 1999, Klemke et al., 1998, Sakai et al., 1994, Sanders et al., 2005, Schaller et al., 1995, Sharma et al., 2008). Thus, the BCAR3 SH2 and Y117 provide a critical switch to activate Cas. Our results also suggest that phosphorylation at Y117 promotes SOCS6 binding and targets BCAR3 for ubiquitination and degradation by the CRL5 E3 ubiquitin ligase. pY-Cas is independently targeted by $CRL5^{SOCS6}$ binding to its pYDYV motif (Teckchandani et al., 2014). Ubiquitination likely occurs within the adhesion (Teckchandani et al., 2016). Ubiquitination and degradation of either protein is expected to terminate signaling until new Cas and BCAR3 molecules are recruited from the cytosol, providing double insurance against excess activity.

Our results reveal that BCAR3 Y117 is required for both signaling and degradation. This means that BCAR3 activation triggers BCAR3 degradation in a negative feedback loop. The dual use of a single site for activation and degradation resembles Y198 of the neuron migration protein Dab1, which binds downstream signaling molecules and also recruits SOCS6/7 for CRL5-

dependent degradation (Simo et al., 2013). Mutating the SOCS-binding site in BCAR3 or Dab1 generates a non-functional protein that accumulates at higher level. In contrast, the SOCS6-binding site in Cas is not needed for downstream signaling, so mutating the site causes increased levels of an active protein and a dominant gain of function phenotype (Teckchandani et al., 2014).

BCAR3 Y117 is conserved across vertebrates, including zebrafish. How might it signal? Its phosphorylation could recruit an SH2 domain protein to stimulate Cas phosphorylation. The Y117 sequence, pYVKF, contains hydrophobic residues at +1 and +3 that characterize other SOCS6 SH2 binding sites (Krebs et al., 2002, Simo et al., 2013, Teckchandani et al., 2014, Zadjali et al., 2011) (Figure 8 – Figure Supplement 3). However, it also contains a lysine residue at position +2 and basic residues tend to inhibit SH2 domain binding (Songyang et al., 1993). Therefore, Y117 phosphorylation may instead stimulate Cas phosphorylation by an allosteric mechanism or by altering binding to other charged molecules, such as membrane phospholipids.

BCAR3 is one of three human NSP proteins. MCF10A cells also express SH2D3A/NSP1, but this protein is not conserved across mammals and lacks a Y117 homolog, so may be unable to functionally substitute for BCAR3. The third family member, SH2D3C/SHEP1, contains a phosphorylated Y117 homolog but is not expressed in MCF10A cells (Vervoort et al., 2007). Likewise, Cas is the only member of its protein family that is significantly expressed in MCF10A cells (http://lincs.hms.harvard.edu/db/datasets/20348/results). Thus, the lack of a Y117 homolog in SH2D3A and the absence of SH2D3C expression could explain why depleting BCAR3 from MCF10A cells phenocopies depletion of Cas.

Our results add to our understanding of how Cas localizes to adhesions, which requires its CCH/FAT domain (Branis et al., 2017, Donato et al., 2010, Janostiak et al., 2014, Nakamoto et al., 1997). While BCAR3 may regulate Cas localization in breast cancer cells and fibroblasts (Makkinje et al., 2009, Schrecengost et al., 2007, Sun et al., 2012), our data suggest that BCAR3 does not regulate Cas localization in normal epithelia. Whether these differences are due to the difference in cell type or expression level is unclear. Other Cas C terminus-binding proteins include paxillin, zyxin and ajuba (Pratt et al., 2005, Yi et al., 2002, Zhang et al., 2017). CCH/FAT binding to paxillin LD motifs in vitro is very weak and predicted to be out-competed by BCAR3 (Zhang et al., 2017). Zyxin was reported to bind to Cas homolog NEDD9 via a

sequence upstream of the NEDD9 CCH/FAT (Yi et al., 2002). However, Cas appears in adhesions before zyxin (Zaidel-Bar et al., 2004). The pre-LIM region of Ajuba binds the Cas CCH/FAT tightly and Cas is mis-localized in ajuba-deficient cells (Pratt et al., 2005). The ajuba LIM domains bind to actin filaments under tension (Winkelman et al., 2020) and localize to adhesions (Pratt et al., 2005). Thus, ajuba or other LIM domain proteins, rather than BCAR3, may be responsible for localizing Cas to adhesions.

Cas phosphorylation requires SFKs, and in some cell types, FAK. Src efficiently phosphorylates Cas in vitro and FAK may act indirectly as an activator and scaffold for Src (Ruest et al., 2001, Sharma et al., 2008). What then is the role of BCAR3? One possibility is that BCAR3 helps activate SFKs in adhesions. Previous studies reported that SFK autophosphorylation is regulated by BCAR3, but the mechanism was unclear (Riggins et al., 2003, Schuh et al., 2010, Sun et al., 2012). In fibroblasts, phosphorylated PTPRA binds to the BCAR3 SH2 domain and brings Cas to FAs for phosphorylation by SFKs (Sun et al., 2012). Since PTPRA is able to activate SFKs by SH2 competition or dephosphorylating a C-terminal inhibitory tyrosine residue (Ponniah et al., 1999, Su et al., 1999, Zheng et al., 2000), this is an attractive model. However, in our studies, the BCAR3 SH2 domain is not needed for BCAR3 or Cas localization, suggesting that Cas-BCAR3 would bring PTPRA to FAs rather than vice versa. In addition, PTPRA is not needed for Cas phosphorylation (data not shown). Therefore, how BCAR3 regulates SFK activity in this system will require further study.

Our finding that BCAR3 is subject to complex post-translational regulation may be helpful in reconciling the observation that BCAR3 over-expression in cell culture increases transformed phenotypes whereas BCAR3 RNA expression correlates with favorable outcomes in patients (Guo et al., 2014, Wallez et al., 2012, Zhang et al., 2018). In addition to the phosphorylation-dependent mechanism investigated here, a previous study showed that TGFβ stimulates proteasomal degradation of BCAR3 (Guo et al., 2014), and over-expressed BCAR3 and Cas appear to stabilize each other in breast cancer cells, dependent on their mutual binding (Wallez et al., 2014). It is possible that changes in BCAR3 protein stability or phosphorylation state influence BCAR3 activity in patients, but that these regulations at the protein level are not accounted for when correlating patient outcomes with gene expression. Thus, further study is required to understand mechanisms of BCAR3 regulation and how mis-regulation may contribute to disease progression.

Materials and Methods

Plasmids

pMXpuroII and pMXpuroII-shCul5 plasmids were made as previously described (Teckchandani et al., 2014). pLKO.1-nontarget small hairpin RNA (shRNA) control vector (SHC002) and pLKO.1-shSOCS6 (TRCN0000284351) were purchased (Sigma Aldrich).

pCAG-T7-mSOCS1, pCAG-T7-mSOCS2, pCAG-T7-mSOCS3, pCAG-T7-mSOCS4, pCAG-T7-mSOCS5, pCAG-T7-mSOCS6, pCAG-T7-mSOCS7, and pCAG-T7-mCisH were made as previously described (Simo et al., 2013, Teckchandani et al., 2014). All pCAG-T7-SOCS plasmids used in this work have LC-QQ mutations in the SOCS box to prevent binding to CRL5, and were made using PfuTurbo DNA polymerase to perform site-directed mutagenesis followed by DpnI digestion. pCAG-T7-mSOCS6 R407K was made as previously described (Teckchandani et al., 2016). pCAG-T7-mSOCS6 ΔC was made by PCR amplifying codons 1-381 of mSOCS6 using a 5' primer complementary to the T7 tag and a 3' primer that inserts a stop codon and a NotI site after codon 381. The PCR product was inserted into pCAG-T7-SOCS6 by BamH1/NotI restriction digest and ligation.

pCMV-SPORT6-mBCAR3 was purchased from the Harvard Plasmid Database (MmCD00318547). pcDNA5-3xFlag-mBCAR3 FRT/TO was made by Gateway cloning. mBCAR3 was PCR amplified with flanking attB sites from pCMV-SPORT6-mBCAR3 and inserted into pDONR221 with a BP reaction (Thermo Fisher Scientific). pDEST-5'-3xFlag-pcDNA FRT/TO was a kind gift of Dr. Anne-Claude Gingras. pDONR221-mBCAR3 was moved into pDEST-5'-3xFlag-pcDNA FRT/TO with a LR reaction (Thermo Fisher Scientific).

pLX304-hBCAR3-V5 was obtained from the human ORFeome version 8.1 Entry clone collection (Yang et al., 2011). pLX304-hBCAR3-F5-V5 was made by Gibson Assembly (New England Biolabs). A gBlock (Integrated DNA Technologies) containing BCAR3 Y42F, Y117F, Y212F, Y266F and Y429F mutations was assembled into pLX304-hBCAR3-V5.

rtTA-N144 was a gift from Andrew Yoo (Addgene plasmid # 66810).

pLTRE3G-SNAP-V5-hBCAR3 was made as follows. A gBlock containing sequence for SNAP-V5 tags was inserted into pLenti CMVTRE3G eGFP Blast (w818-1) (gift of Eric Campenau, Addgene #27568) at the AgeI restriction site using Gibson Assembly to make pLTRE3G-SNAP-

V5-eGFP. hBCAR3 was PCR amplified with flanking AgeI and XbaI sites and inserted into AgeI and XbaI-digested pLTRE3G-SNAP-V5-eGFP to make pLTRE3G-SNAP-V5-hBCAR3.

pLTRE3G-SNAP-V5-hBCAR3 mutants were made as follows. Single mutants Y42F, Y212F, Y266F, Y429F, R177K, and double mutant EE (L744E/R748E) were made by site-directed mutagenesis with Q5 polymerase (New England Biolabs) and Dpn1 digestion. The Y117F mutant was made by Gibson Assembly. A gBlock containing the BCAR3 Y117F mutation was assembled into pLTRE3G-SNAP-V5-hBCAR3 WT. pLTRE3G-SNAP-V5-hBCAR3 F5 was made by BamHI restriction digest of pLTRE3G-SNAP-V5-hBCAR3 Y42F, discarding the region between codon 107 and 763 and inserting the corresponding region from pLX304-hBCAR3-F5-V5. pLTRE3G-SNAP-V5-hBCAR3 F4 was made by PshAI restriction digest of pLTRE3G-SNAP-V5-hBCAR3 F5, discarding the region between codon 67 and 163 inserting the corresponding region from pLTRE3G-SNAP-V5-hBCAR3 WT.

Cell lines

MCF10A cells were cultured in DMEM/F12 (Thermo Fisher Scientific) supplemented with 5% horse serum (Thermo Fisher Scientific), 0.1 μg/ml cholera toxin (EMD Millipore), 10 μg/ml insulin (Thermo Fisher Scientific), 0.5 μg/ml hydrocortisone (Sigma-Aldrich), and 20 ng/ml EGF (Thermo Fisher Scientific). Indicated experiments used assay media (DMEM/F12, 2% horse serum, 0.1 μg/ml cholera toxin, 10 μg/ml insulin, 0.5 μg/ml hydrocortisone, and 0 ng/ml EGF). The cells were passaged using 0.02% trypsin in PBS/EDTA. Trypsin was inactivated with an equal volume of DMEM/10% FBS and cells were harvested by centrifugation before resuspending in growth media. HeLa and 293T cells were grown in DMEM/10% FBS and passaged with trypsin as above.

MCF10A empty vector (EV) and shCul5 cells were made as previously described (Teckchandani et al., 2014). MCF10A shControl and shSOCS6 cells were made as follows. Viruses containing pLKO.1-control and pLKO.1-shSOCS6 were packaged using HEK 293T cells and MCF10A cells were infected. Stable cell lines were selected using 4 µg/mL puromycin.

BCAR3-/- MCF10A cells were made as follows. Early passage MCF10A cells were serially diluted and subclones were grown and characterized. Clone J8 was selected for its epithelial morphology. The J8 clonal cell line was infected with lentiCRISPR v2 (a gift from Feng Zhang; Addgene plasmid # 52961), lacking or containing guide RNA against BCAR3. pLCRISPRv2-

sgRNA-hBCAR3(30) and (31) were made by cloning annealed oligos (5'-CACCGTCAGAGAGCTACCTGCCGAT-3' or 5'-CACCGCCCGAAACATACCAATCGGC-3') into the BsmBI site of plentiCRISPRv2. Potential knockouts were isolated by single cell expansion. Validation of *BCAR3* knockout was done through genomic DNA isolation, PCR, and sequencing, as well as Western blotting.

MCF10A dox-inducible SNAP-V5 BCAR3 cells were made as follows. Viruses containing rtTA-N144 were packaged using 293T cells and used to infect MCF10A cells. A stable line was selected using 50 µg/mL hygromycin. The MCF10A cell line stably expressing rtTA was then infected with viruses containing one of the pLTRE3G-SNAP-V5 constructs (pLTRE3G-SNAP-V5-eGFP, pLTRE3G-SNAP-V5-BCAR3 WT, Y42F, Y117F, Y212F, Y266F, Y429F, F5, F4, R177K, or EE). Stable lines were selected using 10 µg/mL blasticidin. Each cell line was hygromycin resistant and blasticidin resistant, however not all cells within each line expressed the SNAP-V5-containing construct following induction with 50-100ng/mL dox for 48-72 hours. To remove non-inducible cells, dox-treated cells were treated with 100 nM JaneliaFluor cp646JF-SNAP-ligand (Lavis Lab, Janelia Farms) (Grimm et al., 2015) for 1 hour, washed three times with PBS, incubated in ligand-free growth media for an hour and positive cells were sorted and harvested by FACS using the APC channel to detect cp646JF.

Antibodies and Reagents

Antibody	Supplier	Catalog	Dilution
rabbit anti-BCAR3	Bethyl	A301-671A-M	Western (1:2000)
rabbit anti-Cas (C-20)	Santa Cruz	sc-960	Western (1:1000)
mouse anti-Cas	BD Biosciences	610271	Western (1:5000)
rabbit anti-pY165 Cas	Cell Signaling	4015S	IF (1:200)
rabbit anti-Cullin5	Abcam	ab184177	Western (1:1000)
rabbit anti-GAPDH (0411)	Santa Cruz	sc-47724	Western (1:1000)
mouse anti-vinculin	Sigma	V9131	Western (1:10000)
mouse anti-paxillin	BD Biosciences	610051	IF (1:200)
mouse anti-FLAG	Sigma	F1804	Western (1:1000)

mouse anti-T7	EMB Biosciences	69522-4	Western (1:5000) IP
rabbit anti-V5	Bethyl	A190-120A	Western (1:5000) IP
AlexaFluor 488 goat anti-rabbit IgG (H+L)	Invitrogen	A11008	IF (1:1000)
AlexaFluor 647 goat anti-mouse IgG (H+L)	Invitrogen	A28181	IF (1:1000)

Reagents used: cycloheximide (Sigma), epidermal growth factor (Invitrogen), MLN4924 (Active Biochem), MG132 (Fisher Scientific), bafilomycin A, doxycycline (Fisher Scientific).

Mass spectrometry

MCF10A EV and shCul5 cells were grown in 15-cm plates, two plates per condition, to approximately 80% confluence, washed in PBS, and lysed in 3 mL per plate of ice-cold 8 M urea containing 1 mM sodium orthovanadate. Proteins were reduced, alkylated and digested with trypsin as described (Zhang et al., 2005). Peptide labeling with iTRAQ reagents (TMT 6plex, Themo Fisher Scientific) was performed according to the manufacturer's instructions, using 400 μg of each sample. After reaction, the six samples were combined and concentrated under vacuum. For immunoprecipitation, protein G agrarose (60 μl, Millipore) was incubated with anti-phosphotyrosine antibodies (12 μg 4G10 (Millipore), 12 μg PT66 (Sigma) and 12 μg PY100 (Cell Signaling Technology) for 8 hours at 4 ^{o}C with rotation, then washed with 400 μl IP buffer (100 mM Tris HCl, 100 mM NaCl, and 1 % Nonidet P-40, pH 7.4). The TMT-labeled peptides were resuspended in 400 μl IP buffer and pH adjusted to 7.4, then mixed with the antibody-conjugated protein G agarose overnight at 4 ^{o}C with rotation. The antibody beads were spun down and the supernatant saved. The beads were washed with 400 μl IP buffer then four rinses with 100 mM Tris HCl pH 7.4 before elution with 70 μl of 100 mM glycine, pH 2.0 for 30 minutes at 25 ^{o}C. Offline immobilized metal affinity chromatography (IMAC) was used to further enrich for phosphotyrosine peptides (Zhang et al., 2005).

Peptides were loaded on a precolumn and separated by reverse phase HPLC using an EASY-nLC1000 (Thermo) over a 140-minute gradient from 100% solvent A (H_2O/CH_3COOH, 99:1 (v/v)) to 30% A: 70% B ($H_2O/CH_3CN/CH_3COOH$, 29:70:1 (v/v)). Eluted peptides were injected

using nanoelectrospray into a QExactive Pluss mass spectrometer (Thermo) in data-dependent mode. The parameters for full scan MS were: resolution of 70,000 across 350-2000 *m/z*, AGC $3e^6$, and maximum IT 50 ms. The full MS scan was followed by MS/MS for the top 10 precursor ions in each cycle with a NCE of 34 and dynamic exclusion of 30 s. Raw mass spectral files (.raw) were searched using Proteome Discoverer (Thermo) and Mascot version 2.4.1 (Matrix Science). Mascot search parameters were: 10 ppm mass tolerance for precursor ions; 15 mmu for fragment ion mass tolerance; 2 missed cleavages of trypsin; fixed modifications were carbamidomethylation of cysteine and TMT 6plex modification of lysines and peptide N-termini; variable modifications were methionine oxidation, tyrosine, serine and threonine phosphorylation. TMT quantification was obtained using Proteome Discoverer and isotopically corrected per manufacturer's directions, and normalized to the mean relative protein quantification ratios obtained from the total protein analysis (0.2% of the unbound peptides from the phosphotyrosine peptide immunoprecipitation). Mascot peptide identifications, phosphorylation site assignments and quantification were verified manually with the assistance of CAMV (Curran et al., 2013). Validated data were analyzed in Excel using a one-sided two-sample equal variance Student t-test.

siRNA Transfection

MCF10A cells were trypsinized and seeded in growth medium into a 12-well plate so as to be 50% confluent after attaching. A mixture of 50 pmol siRNA, 1.25 μl Lipofectamine 2000 (Invitrogen) in Optimem medium (Invitrogen) was added to the newly plated MCF10A cells and left for the cells to attach overnight. The next day the media was changed to fresh growth media. A second siRNA transfection was done 48 hours after the first transfection using the same protocol scaled up to use a 6-well plate (125 pmol siRNA) or scaled down to use a 96-well plate (for migration assays). One day later, cells from the 6-well dish were transferred to 4-well plates containing 12-mm coverslips for microscopy, or 12-well plates for protein analysis. Doxycline was added as needed at 10 ng/mL for 2-3 days before analysis. Cells were either lysed 48 hours after the second transfection or assays were performed as described.

siRNA	Target Sequence	Source	Notes	Catalog
Control siRNA	5'-AATTCTCCCGAACGTGTCACGT-3'	Qiagen		1027310
SOCS6 siRNA Pool	5'-TAGAATCGTGAATTGACATAA-3' 5'-CAGCTGCGATATCAACGGTGA-3'	Qiagen		SI00061383 SI03068359

	5'-TTGATCTAATTGAGCATTCAA-3' 5'-CGGGTACAAATTGGCATAACA-3'			SI00061369 SI00061376
Cul5 siRNA Pool	5'-GACACGACGTCTTATATTA-3' 5'-CGTCTAATCTGTTAAAGAA-3' 5'-GATGATACGGCTTTGCTAA-3' 5'-GTTCAACTACGAATACTAA-3'	GE Dharmacon		M-019553-01-0005
BCAR1 siRNA Pool	5'-AAGCAGTTTGAACGACTGGAA-3' 5'-CTGGATGGAGGACTATGACTA-3' 5'-CAGCATCACGCGGCAGGGCAA-3' 5'-CAACCTGACCACACTGACCAA-3'	Qiagen		SI02757741 SI02757734 SI04438280 SI04438273
BCAR3 siRNA Pool	5'-CCGGAACTCTGGCGTCAACTA-3' 5'-CCGAGCGGCCACTCTGAGTAA-3' 5'-GCCCAACGAGTTTGAGTCAAA-3' 5'-AAGGTATCAGTTATATGATAT-3'	Qiagen		SI03081603 SI03080196 SI00053102 SI00053095
BCAR3 siRNA	5'-GGUAACUACUGCUAAUGUUTT-3'	Life Technologies	Targets 3'UTR	AM16708

qPCR

An RNeasy Plus Mini kit (Qiagen) was used to extract RNA and an iScript reverse transcription supermix (BioRad) was used to make cDNA. Control reactions lacked reverse transcriptase. cDNA abundance was measured using an iTaq Universal SYBR Green Supermix kit (BioRad). Samples were run on the QuantStudio 5 Real-Time PCR System.

Primer	Sequence
BCAR3 forward	5' – AATCGCTTCTCCAAACAGAGC – 3'
BCAR3 reverse	5' – ATTCACCGGCATGTTTCTGG – 3'
Cul5 forward	5' – TTTTATGCGCCCGATTGTTTTG – 3'
Cul5 reverse	5' – TTGCTGGGCCTTTATCATCCC – 3'
GAPDH forward	5' – CAGCCTCAAGATCATCAGCA – 3'
GAPDH reverse	5' – TGTGGTCATGAGTCCTTCCA – 3'

Cell lysis and Immunoblotting

Cells were washed three times in phosphate-buffered saline (PBS) before lysis. Cells were lysed in X-100 buffer (1% Triton X-100, 150 mM NaCl, 10 mM HEPES pH 7.4, 2 mM EDTA, 50 mM NaF) or RIPA buffer (1% Triton X-100, 1% sodium deoxycholate, 0.1% SDS, 20 mM Tris-HCl pH 7.4, 150 mM NaCl, 5 mM EDTA, 5 mM EGTA) with fresh protease and phosphatase inhibitors (10 μg/mL Aprotinin, 1 mM PMSF, 1 mM sodium vanadate) added before use.

Lysates were adjusted to SDS sample buffer, heated to 95 °C, resolved by SDS-PAGE using 10% polyacrylamide/0.133% bis-acrylamide gels, and transferred onto nitrocellulose membrane. The membrane was blocked in Odyssey blocking buffer (TBS) (LI-COR Biosciences) with 5% BSA for phosphotyrosine antibodies or 5% non-fat dry milk for all other antibodies. Following blocking, the membrane was probed with a primary antibody followed by IRDye 800CW goat anti-rabbit or 680RD goat anti-mouse conjugated secondary antibodies. Membranes were visualized using the Odyssey Infrared Imaging System (LI-COR Biosciences).

DNA transfections and Immunoprecipitation

HeLa cells were plated in 6-well plates the day before transfection such that cells were 50% confluent on the day of transfection. A mixture of DNA, Lipofectamine 2000 (Thermo Fisher Scientific) and Optimem (Invitrogen) was made according to manufacturer's protocol, added to the cells and removed after 5 hours.

Immunoprecipitation experiments were conducted 24-48 hours after transfection. For indicated experiments, cells were incubated with 1 mM sodium pervanadate for 30 minutes. Cells were lysed on ice in X-100 buffer with fresh protease and phosphatase inhibitors (see above). Lysates were cleared by centrifugation for 10 minutes at 14,000 g. Lysates were rotated with 1 μg antibody at 4°C for 3 hours, after which Protein A/G plus agarose beads (Santa Cruz Biotechnology) were added for 1 hour at 4°C. Beads were collected by centrifugation and washed three times with X-100 buffer. The beads were resuspended in SDS sample buffer, boiled, lightly mixed to release bound protein and centrifuged. Immunoprecipitation samples were resolved by SDS-PAGE using 10% polyacrylamide gels and bound proteins detected by Western blotting as above. Samples of total cell lysate typically contained 5% of the protein used for immunoprecipitation.

Cycloheximide chase

Cells were grown to 80% confluency and treated with 25μg/mL cycloheximide by adding it directly to the conditioned media on the cells. Cells were treated with cycloheximide for 0, 2, 4, or 8 hours and lysed. Quantification of Western blots was done in ImageJ and BCAR3 protein levels were normalized to the loading control (GAPDH or vinculin).

Scratch wound assay

The desired proteins were knocked down using two siRNA transfections, as previously described. Cells were plated in ImageLock 96-well dishes (Essen BioScience) for the second siRNA transfection and transfection materials were scaled down proportional to dish sizes. Cells were plated at 30% confluence at the time of the second transfection. For migration assays where doxycycline (dox)-induction was required, the media was replaced with growth media containing dox (10 ng/mL except where noted) 6 hours after transfection and after two washes with PBS. For all migration assays, the confluent monolayers were placed in EGF-free assay media (with dox when required) 48 hours after the second transfection transfection. Monolayers were scratched using an Incucyte WoundMaker (Essen BioScience) 8 hours after being placed in assay media, the wells were washed with PBS three times to remove debris and cells were placed back in assay media (with dox when required). Scratch wounds were imaged once every 2 hours on an IncuCyte S3 and images were analyzed using the scratch wound function on the IncuCyte image analysis software. Overall migration was measured using the relative wound density calculated by the analysis software. Lamellipodium length was measured using the ruler in the IncuCyte image analysis software. Membrane ruffles were visualized as dark contrast at the front of the protrusion. Ruffling was scored by counting the number of leading edge cells that did and did not have membrane ruffles to calculate a percentage of ruffling cells.

Transwell migration and invasion assays

Cells were grown in EGF-free assay media for 24 hours before the assay. Migration assays were performed in 24-well chemotaxis chamber with an 8 μm pore size polyethylene terephthalate filter that separated the upper and lower wells (Thermo Fisher Scientific). Invasion assays were performed in 24-well Matrigel invasion chambers with an 8 μm pore size polyethylene terephthalate filter coated in Matrigel matrix that separated the upper and lower wells (Thermo Fisher Scientific). In both assays, the lower wells were filled with MCF10A growth media. 80,000 cells were resuspended in EGF-free assay media and added to the top well. After 24 hours, cells on the top of the membrane were removed and the cells on the bottom of

the membrane were fixed with methanol and stained with SybrSafe at 1:10,000 for 15 minutes. Membranes were rinsed, imaged and nuclei were counted.

Immunofluorescence

For experiments that required protein knockdown, cells were transfected with siRNA as previously described. On the day following the second siRNA transfection, cells were plated on 12-mm #1.5 coverslips at 30% confluency in 4-well or 24-well (1.9 cm^2) plates for scratch wound assays (with dox when required). Cells were placed in assay media overnight the day before the assay and confluent monolayers were scratched with a P200 pipette tip the following morning. Cells were fixed and permeabilized 6 hours after the start of migration.

To detect the SNAP tag, JaneliaFluor cpJF549 SNAP-ligand (Lavis Lab, Janelia Farms) (Grimm et al., 2015) was added to the cells at 100 nM 4 hours after forming the wounds. Cells were incubated for 1 hour with the SNAP-ligand, washed three times with PBS and placed in fresh, ligand-free assay media for 1 hour to remove unreacted SNAP-ligand.

Fixation and immunostaining was done at room temperature. Cells were washed with PBS, fixed and permeabilized with 0.1% Triton X-100, 4% paraformaldehyde (PFA) in PBS for 2 minutes, and further fixed with 4% PFA/PBS for 15 minutes. Cells were blocked with 2% BSA, 5% normal goat serum in PBS for 30 minutes or overnight at 4°C. Primary antibodies were diluted in block solution (typically 1:200 dilution) and added for 3 hours. Coverslips were washed three times with PBS. AlexaFluor-labeled secondary antibodies, diluted 1:1000 in PBS, were added for 1 hour. Coverslips were washed three times with PBS, mounted in Prolong Glass Antifade Mountant and left to cure overnight in the dark before imaging or storing in the cold.

Imaging and image quantification

Coverslips were imaged using 63x, 1.40 NA or 100x, 1.40 NA oil objectives on a Leica SP8 confocal microscope and deconvolved using Leica LAS acquisition software. Scale and imaging settings were consistent within each experiment.

Image quantification was done in ImageJ. A line was drawn ~6 μm from the front of the migrating cells, as described (Teckchandani et al., 2016), to isolate the leading edge. Using the threshold tool on ImageJ, paxillin-containing adhesions were identified and mean intensity of SNAP, pY-Cas, EYFP-Cas and paxillin in these leading edge adhesions and in the cytoplasm at

the rear of the cell were calculated. The SNAP/paxillin ratio was calculated by subtracting a ligand background mean intensity value (taken from a non-dox-induced sample) from the SNAP mean intensity, normalizing to the cytoplasmic SNAP mean intensity and then dividing by the paxillin mean intensity that was normalized to cytoplasmic paxillin mean intensity. The EYFP-Cas/paxillin ratio was calculated by normalizing the mean intensities of each in adhesions to the mean intensities in the cytoplasm and dividing normalized EYFP-Cas intensity by the normalized paxillin intensity. The pY-Cas/paxillin ratio was calculated by dividing the mean intensity of pY-Cas in adhesions by the mean intensity of paxillin.

Acknowledgements

We are most grateful to Forest White for advice on quantitative phosphotyrosine proteomics and Amanda Del Rosario of the Koch Institute Proteomics Core for running the analysis. Julio Vazquez, Dave McDonald, Lena Schroeder and Peng Guo of the FHCRC Cellular Imaging Shared Resource provided outstanding assistance with microscopy. We thank Patrick Paddison, Anne-Claude Gingras and Susumu Antoku for plasmids and Luke Lavis for Janelia Fluors. Laura Arguedas-Jiminez provided excellent technical assistance. We are grateful to Saurav Kumar and Dayoung Kim for discussion and helpful comments on the paper.

E.S. was supported in part by Predoctoral Institutional Training Program T32 GM007270 to the University of Washington. This work was supported by research grant R01 GM109463 from the US Public Health Service and by discretionary funds from the Fred Hutchinson Cancer Research Center. The FHCRC Flow Cytometry and Cellular Imaging Shared Resources are supported by P30 CA015704. The Koch Institute Proteomics Core is supported by P30 CA14051.

Bachir AI, Horwitz AR, Nelson WJ, Bianchini JM. 2017. Actin-based adhesion modules mediate cell interactions with the extracellular matrix and neighboring cells. *Cold Spring Harb Perspect Biol* **9**. doi: 10.1101/cshperspect.a023234.

Baron U, Gossen M, Bujard H. 1997. Tetracycline-controlled transcription in eukaryotes: novel transactivators with graded transactivation potential. *Nucleic Acids Res* **25**:2723-9.

Bayle J, Letard S, Frank R, Dubreuil P, De Sepulveda P. 2004. Suppressor of cytokine signaling 6 associates with KIT and regulates KIT receptor signaling. *J Biol Chem* **279**:12249-59. doi: 10.1074/jbc.M313381200.

Boettner B, Van Aelst L. 2009. Control of cell adhesion dynamics by Rap1 signaling. *Curr Opin Cell Biol* **21**:684-93.

Branis J, Pataki C, Sporrer M, Gerum RC, Mainka A, Cermak V, Goldmann WH, Fabry B, Brabek J, Rosel D. 2017. The role of focal adhesion anchoring domains of CAS in mechanotransduction. *Sci Rep* **7**:46233. doi: 10.1038/srep46233.

Burridge K, Turner CE, Romer LH. 1992. Tyrosine phosphorylation of paxillin and pp125FAK accompanies cell adhesion to extracellular matrix: a role in cytoskeletal assembly. *J Cell Biol* **119**:893-903.

Cai D, Clayton LK, Smolyar A, Lerner A. 1999. AND-34, a novel p130Cas-binding thymic stromal cell protein regulated by adhesion and inflammatory cytokines. *J Immunol* **163**:2104-12.

Cai D, Iyer A, Felekkis KN, Near RI, Luo Z, Chernoff J, Albanese C, Pestell RG, Lerner A. 2003. AND-34/BCAR3, a GDP exchange factor whose overexpression confers antiestrogen resistance, activates Rac, PAK1, and the cyclin D1 promoter. *Cancer Res* **63**:6802-8.

Case LB, Waterman CM. 2015. Integration of actin dynamics and cell adhesion by a three-dimensional, mechanosensitive molecular clutch. *Nat Cell Biol*. doi: 10.1038/ncb3191.

Cheresh DA, Leng J, Klemke RL. 1999. Regulation of cell contraction and membrane ruffling by distinct signals in migratory cells. *J Cell Biol* **146**:1107-16.

Cross AM, Wilson AL, Guerrero MS, Thomas KS, Bachir AI, Kubow KE, Horwitz AR, Bouton AH. 2016. Breast cancer antiestrogen resistance 3-p130(Cas) interactions promote adhesion disassembly and invasion in breast cancer cells. *Oncogene* **35**:5850-5859. doi: 10.1038/onc.2016.123.

Curran TG, Bryson BD, Reigelhaupt M, Johnson H, White FM. 2013. Computer aided manual validation of mass spectrometry-based proteomic data. *Methods* **61**:219-26. doi: 10.1016/j.ymeth.2013.03.004.

Defilippi P, Di Stefano P, Cabodi S. 2006. p130Cas: a versatile scaffold in signaling networks. *Trends Cell Biol* **16**:257-63.

del Rio A, Perez-Jimenez R, Liu R, Roca-Cusachs P, Fernandez JM, Sheetz MP. 2009. Stretching single talin rod molecules activates vinculin binding. *Science* **323**:638-41. doi: 10.1126/science.1162912.

DeMali KA, Barlow CA, Burridge K. 2002. Recruitment of the Arp2/3 complex to vinculin: coupling membrane protrusion to matrix adhesion. *J Cell Biol* **159**:881-91.

Donato DM, Ryzhova LM, Meenderink LM, Kaverina I, Hanks SK. 2010. Dynamics and mechanism of p130Cas localization to focal adhesions. *J Biol Chem* **285**:20769-79. doi: 10.1074/jbc.M109.091207.

Feng L, Cooper JA. 2009. Dual functions of Dab1 during brain development. *Mol Cell Biol* **29**:324-32.

Fonseca PM, Shin NY, Brabek J, Ryzhova L, Wu J, Hanks SK. 2004. Regulation and localization of CAS substrate domain tyrosine phosphorylation. *Cell Signal* **16**:621-9.

Galbraith CG, Yamada KM, Sheetz MP. 2002. The relationship between force and focal complex development. *J Cell Biol* **159**:695-705. doi: 10.1083/jcb.200204153.

Goldberg GS, Alexander DB, Pellicena P, Zhang ZY, Tsuda H, Miller WT. 2003. Src phosphorylates Cas on tyrosine 253 to promote migration of transformed cells. *J Biol Chem* **278**:46533-40.

Grimm JB, English BP, Chen J, Slaughter JP, Zhang Z, Revyakin A, Patel R, Macklin JJ, Normanno D, Singer RH, Lionnet T, Lavis LD. 2015. A general method to improve fluorophores for live-cell and single-molecule microscopy. *Nat Methods* **12**:244-50, 3 p following 250. doi: 10.1038/nmeth.3256.

Guo J, Canaff L, Rajadurai CV, Fils-Aime N, Tian J, Dai M, Korah J, Villatoro M, Park M, Ali S, Lebrun JJ. 2014. Breast cancer anti-estrogen resistance 3 inhibits transforming growth factor beta/Smad signaling and associates with favorable breast cancer disease outcomes. *Breast Cancer Res* **16**:476. doi: 10.1186/s13058-014-0476-9.

Harte MT, Hildebrand JD, Burnham MR, Bouton AH, Parsons JT. 1996. p130Cas, a substrate associated with v-Src and v-Crk, localizes to focal adhesions and binds to focal adhesion kinase. *J Biol Chem* **271**:13649-55. doi: 10.1074/jbc.271.23.13649.

Hasegawa H, Kiyokawa E, Tanaka S, Nagashima K, Gotoh N, Shibuya M, Kurata T, Matsuda M. 1996. DOCK180, a major CRK-binding protein, alters cell morphology upon translocation to the cell membrane. *Mol Cell Biol* **16**:1770-6.

Honda H, Nakamoto T, Sakai R, Hirai H. 1999. p130(Cas), an assembling molecule of actin filaments, promotes cell movement, cell migration, and cell spreading in fibroblasts. *Biochem Biophys Res Commun* **262**:25-30.

Hornbeck PV, Kornhauser JM, Latham V, Murray B, Nandhikonda V, Nord A, Skrzypek E, Wheeler T, Zhang B, Gnad F. 2019. 15 years of PhosphoSitePlus(R): integrating post-translationally modified sites, disease variants and isoforms. *Nucleic Acids Res* **47**:D433-D441. doi: 10.1093/nar/gky1159.

Hotta K, Ranganathan S, Liu R, Wu F, Machiyama H, Gao R, Hirata H, Soni N, Ohe T, Hogue CW, Madhusudhan MS, Sawada Y. 2014. Biophysical properties of intrinsically disordered p130Cas substrate domain--implication in mechanosensing. *PLoS Comput Biol* **10**:e1003532. doi: 10.1371/journal.pcbi.1003532.

Huang MM, Lipfert L, Cunningham M, Brugge JS, Ginsberg MH, Shattil SJ. 1993. Adhesive ligand binding to integrin alpha IIb beta 3 stimulates tyrosine phosphorylation of novel protein substrates before phosphorylation of pp125FAK. *J Cell Biol* **122**:473-83.

Jaber Chehayeb R, Boggon TJ. 2020. SH2 Domain Binding: Diverse FLVRs of Partnership. *Front Endocrinol (Lausanne)* **11**:575220. doi: 10.3389/fendo.2020.575220.

Janostiak R, Brabek J, Auernheimer V, Tatarova Z, Lautscham LA, Dey T, Gemperle J, Merkel R, Goldmann WH, Fabry B, Rosel D. 2014. CAS directly interacts with vinculin to control mechanosensing and focal adhesion dynamics. *Cell Mol Life Sci* **71**:727-44. doi: 10.1007/s00018-013-1450-x.

Kazi JU, Sun J, Phung B, Zadjali F, Flores-Morales A, Ronnstrand L. 2012. Suppressor of cytokine signaling 6 (SOCS6) negatively regulates Flt3 signal transduction through direct binding to phosphorylated tyrosines 591 and 919 of Flt3. *J Biol Chem* **287**:36509-17. doi: 10.1074/jbc.M112.376111.

Keppler A, Gendreizig S, Gronemeyer T, Pick H, Vogel H, Johnsson K. 2003. A general method for the covalent labeling of fusion proteins with small molecules in vivo. *Nat Biotechnol* **21**:86-9. doi: 10.1038/nbt765.

Kiyokawa E, Hashimoto Y, Kobayashi S, Sugimura H, Kurata T, Matsuda M. 1998. Activation of Rac1 by a Crk SH3-binding protein, DOCK180. *Genes Dev* **12**:3331-6.

Klemke RL, Leng J, Molander R, Brooks PC, Vuori K, Cheresh DA. 1998. CAS/Crk coupling serves as a "molecular switch" for induction of cell migration. *J Cell Biol* **140**:961-72.

Kostic A, Sheetz MP. 2006. Fibronectin rigidity response through Fyn and p130Cas recruitment to the leading edge. *Mol Biol Cell* **17**:2684-95.

Krebs DL, Uren RT, Metcalf D, Rakar S, Zhang JG, Starr R, De Souza DP, Hanzinikolas K, Eyles J, Connolly LM, Simpson RJ, Nicola NA, Nicholson SE, Baca M, Hilton DJ, Alexander WS. 2002. SOCS-6 binds to insulin receptor substrate 4, and mice lacking the SOCS-6 gene exhibit mild growth retardation. *Mol Cell Biol* **22**:4567-78.

Legate KR, Wickstrom SA, Fassler R. 2009. Genetic and cell biological analysis of integrin outside-in signaling. *Genes Dev* **23**:397-418. doi: 10.1101/gad.1758709.

Mace PD, Wallez Y, Dobaczewska MK, Lee JJ, Robinson H, Pasquale EB, Riedl SJ. 2011. NSP-Cas protein structures reveal a promiscuous interaction module in cell signaling. *Nat Struct Mol Biol* **18**:1381-7. doi: 10.1038/nsmb.2152.

Makkinje A, Near RI, Infusini G, Vanden Borre P, Bloom A, Cai D, Costello CE, Lerner A. 2009. AND-34/BCAR3 regulates adhesion-dependent p130Cas serine phosphorylation and breast cancer cell growth pattern. *Cell Signal* **21**:1423-35. doi: 10.1016/j.cellsig.2009.05.006.

Marengere LE, Pawson T. 1994. Structure and function of SH2 domains. *J Cell Sci Suppl* **18**:97-104. doi: 10.1242/jcs.1994.supplement_18.14.

Mitra SK, Schlaepfer DD. 2006. Integrin-regulated FAK-Src signaling in normal and cancer cells. *Curr Opin Cell Biol* **18**:516-23.

Miyamoto S, Teramoto H, Coso OA, Gutkind JS, Burbelo PD, Akiyama SK, Yamada KM. 1995. Integrin function: molecular hierarchies of cytoskeletal and signaling molecules. *J Cell Biol* **131**:791-805.

Nakamoto T, Sakai R, Honda H, Ogawa S, Ueno H, Suzuki T, Aizawa S, Yazaki Y, Hirai H. 1997. Requirements for localization of p130cas to focal adhesions. *Mol Cell Biol* **17**:3884-97.

Nojima Y, Morino N, Mimura T, Hamasaki K, Furuya H, Sakai R, Sato T, Tachibana K, Morimoto C, Yazaki Y, Hirai H. 1995. Integrin-mediated cell adhesion promotes tyrosine phosphorylation of p130Cas, a Src homology 3-containing molecule having multiple Src homology 2-binding motifs. *Journal of Biological Chemistry* **270**:15398-15402.

Oh MJ, van Agthoven T, Choi JE, Jeong YJ, Chung YH, Kim CM, Jhun BH. 2008. BCAR3 regulates EGF-induced DNA synthesis in normal human breast MCF-12A cells. *Biochem Biophys Res Commun* **375**:430-4. doi: 10.1016/j.bbrc.2008.08.040.

Oh MJ, Yi SJ, Kim HS, Kim JH, Jeong YH, van Agthoven T, Jhun BH. 2013. Functional roles of BCAR3 in the signaling pathways of insulin leading to DNA synthesis, membrane ruffling and GLUT4 translocation. *Biochem Biophys Res Commun* **441**:911-6. doi: 10.1016/j.bbrc.2013.10.161.

Okumura F, Joo-Okumura A, Nakatsukasa K, Kamura T. 2016. The role of cullin 5-containing ubiquitin ligases. *Cell Div* **11**:1. doi: 10.1186/s13008-016-0016-3.

Partridge MA, Marcantonio EE. 2006. Initiation of attachment and generation of mature focal adhesions by integrin-containing filopodia in cell spreading. *Mol Biol Cell* **17**:4237-48.

Pasapera AM, Schneider IC, Rericha E, Schlaepfer DD, Waterman CM. 2010. Myosin II activity regulates vinculin recruitment to focal adhesions through FAK-mediated paxillin phosphorylation. *J Cell Biol* **188**:877-90. doi: 10.1083/jcb.200906012.

Polte TR, Hanks SK. 1995. Interaction between focal adhesion kinase and Crk-associated kinase substrate p130cas. *Proceedings of the National Academy of Sciences of the United States of America* **92**:10678-10682.

Ponniah S, Wang DZ, Lim KL, Pallen CJ. 1999. Targeted disruption of the tyrosine phosphatase PTPalpha leads to constitutive downregulation of the kinases Src and Fyn. *Curr Biol* **9**:535-8.

Pratt SJ, Epple H, Ward M, Feng Y, Braga VM, Longmore GD. 2005. The LIM protein Ajuba influences p130Cas localization and Rac1 activity during cell migration. *J Cell Biol* **168**:813-24.

Puklin-Faucher E, Sheetz MP. 2009. The mechanical integrin cycle. *J Cell Sci* **122**:179-86. doi: 10.1242/jcs.042127.

Ren XD, Kiosses WB, Sieg DJ, Otey CA, Schlaepfer DD, Schwartz MA. 2000. Focal adhesion kinase suppresses Rho activity to promote focal adhesion turnover. *J Cell Sci* **113 (Pt 20)**:3673-8.

Ridley AJ. 2001. Rho GTPases and cell migration. *J Cell Sci* **114**:2713-22.

Ridley AJ, Paterson HF, Johnston CL, Diekmann D, Hall A. 1992. The small GTP-binding protein rac regulates growth factor-induced membrane ruffling. *Cell* **70**:401-410.

Riggins RB, Quilliam LA, Bouton AH. 2003. Synergistic promotion of c-Src activation and cell migration by Cas and AND-34/BCAR3. *J Biol Chem* **278**:28264-73. doi: 10.1074/jbc.M303535200.

Roselli S, Wallez Y, Wang L, Vervoort V, Pasquale EB. 2010. The SH2 domain protein Shep1 regulates the in vivo signaling function of the scaffolding protein Cas. *Cell Signal* **22**:1745-52. doi: 10.1016/j.cellsig.2010.06.015.

Rottner K, Hall A, Small JV. 1999. Interplay between Rac and Rho in the control of substrate contact dynamics. *Curr Biol* **9**:640-8.

Ruest PJ, Shin NY, Polte TR, Zhang X, Hanks SK. 2001. Mechanisms of CAS substrate domain tyrosine phosphorylation by FAK and Src. *Mol Cell Biol* **21**:7641-52. doi: 10.1128/MCB.21.22.7641-7652.2001.

Sakai R, Iwamatsu A, Hirano N, Ogawa S, Tantaka T, Mano H, Yazaki Y, Hirai H. 1994. A novel signaling molecule, p130, forms stable complexes in vivo with v-Crk and v-Src in a tyrosine phosphorylation-dependent manner. *EMBO Journal* **13**:3748-3756.

Sakai R, Nakamoto T, Ozawa K, Aizawa S, Hirai H. 1997. Characterization of the kinase activity essential for tyrosine phosphorylation of p130Cas in fibroblasts. *Oncogene* **14**:1419-26. doi: 10.1038/sj.onc.1200954.

Sanders MA, Basson MD. 2005. p130cas but not paxillin is essential for Caco-2 intestinal epithelial cell spreading and migration on collagen IV. *J Biol Chem* **280**:23516-22.

Sawada Y, Tamada M, Dubin-Thaler BJ, Cherniavskaya O, Sakai R, Tanaka S, Sheetz MP. 2006. Force sensing by mechanical extension of the Src family kinase substrate p130Cas. *Cell* **127**:1015-26.

Schaller MD, Borgman CA, Cobb BS, Vines RR, Reynolds AB, Parsons JT. 1992. pp125FAK a structurally distinctive protein-tyrosine kinase associated with focal adhesions. *Proc Natl Acad Sci U S A* **89**:5192-6. doi: 10.1073/pnas.89.11.5192.

Schaller MD, Parsons JT. 1995. pp125FAK-dependent tyrosine phosphorylation of paxillin creates a high-affinity binding site for Crk. *Molecular and Cellular Biology* **15**:2635-2645.

Schrecengost RS, Riggins RB, Thomas KS, Guerrero MS, Bouton AH. 2007. Breast cancer antiestrogen resistance-3 expression regulates breast cancer cell migration through promotion of p130Cas membrane localization and membrane ruffling. *Cancer Res* **67**:6174-82. doi: 10.1158/0008-5472.CAN-06-3455.

Schuh NR, Guerrero MS, Schrecengost RS, Bouton AH. 2010. BCAR3 regulates Src/p130 Cas association, Src kinase activity, and breast cancer adhesion signaling. *J Biol Chem* **285**:2309-17. doi: 10.1074/jbc.M109.046631.

Sharma A, Mayer BJ. 2008. Phosphorylation of p130Cas initiates Rac activation and membrane ruffling. *BMC Cell Biol* **9**:50.

Simo S, Cooper JA. 2013. Rbx2 regulates neuronal migration through different cullin 5-RING ligase adaptors. *Dev Cell* **27**:399-411. doi: 10.1016/j.devcel.2013.09.022.

Songyang Z, Shoelson SE, Chaudhuri M, Gish G, Pawson T, Haser WG, King F, Roberts T, Ratnofsky S, Lechleider RJ, Neel BG, Birge RB, Fajardo JE, Chou MM, Hanafusa H, Schaffhausen B, Cantley LC. 1993. SH2 domains recognize specific phosphopeptide sequences. *Cell* **72**:767-778.

Stradal TE, Rottner K, Disanza A, Confalonieri S, Innocenti M, Scita G. 2004. Regulation of actin dynamics by WASP and WAVE family proteins. *Trends Cell Biol* **14**:303-11.

Stutchbury B, Atherton P, Tsang R, Wang DY, Ballestrem C. 2017. Distinct focal adhesion protein modules control different aspects of mechanotransduction. *J Cell Sci* **130**:1612-1624. doi: 10.1242/jcs.195362.

Su J, Muranjan M, Sap J. 1999. Receptor protein tyrosine phosphatase alpha activates Src-family kinases and controls integrin-mediated responses in fibroblasts. *Curr Biol* **9**:505-11.

Sun G, Cheng SY, Chen M, Lim CJ, Pallen CJ. 2012. Protein tyrosine phosphatase alpha phosphotyrosyl-789 binds BCAR3 to position Cas for activation at integrin-mediated focal adhesions. *Mol Cell Biol* **32**:3776-89. doi: 10.1128/MCB.00214-12.

Tadokoro S, Shattil SJ, Eto K, Tai V, Liddington RC, de Pereda JM, Ginsberg MH, Calderwood DA. 2003. Talin binding to integrin beta tails: a final common step in integrin activation. *Science* **302**:103-6.

Tamada M, Sheetz MP, Sawada Y. 2004. Activation of a signaling cascade by cytoskeleton stretch. *Dev Cell* **7**:709-18.

Tanaka S, Morishita T, Hashimoto Y, Hattori S, Nakamura S, Shibuya M, Matuoka K, Takenawa T, Kurata T, Nagashima K, Matsuda M. 1994. C3G, a guanine nucleotide-releasing protein expressed ubiquitously, binds to the Src homology 3 domains of CRK and GRB2/ASH proteins. *Proc Natl Acad Sci U S A* **91**:3443-7.

Teckchandani A, Cooper JA. 2016. The ubiquitin-proteasome system regulates focal adhesions at the leading edge of migrating cells. *Elife* **5**. doi: 10.7554/eLife.17440.

Teckchandani A, Laszlo GS, Simo S, Shah K, Pilling C, Strait AA, Cooper JA. 2014. Cullin 5 destabilizes Cas to inhibit Src-dependent cell transformation. *J Cell Sci* **127**:509-20. doi: 10.1242/jcs.127829.

Tikhmyanova N, Little JL, Golemis EA. 2010. CAS proteins in normal and pathological cell growth control. *Cell Mol Life Sci* **67**:1025-48. doi: 10.1007/s00018-009-0213-1.

Trepat X, Chen Z, Jacobson K. 2012. Cell migration. *Compr Physiol* **2**:2369-92. doi: 10.1002/cphy.c110012.

van Agthoven T, van Agthoven TL, Dekker A, van der Spek PJ, Vreede L, Dorssers LC. 1998. Identification of BCAR3 by a random search for genes involved in antiestrogen resistance of human breast cancer cells. *EMBO J* **17**:2799-808. doi: 10.1093/emboj/17.10.2799.

Vervoort VS, Roselli S, Oshima RG, Pasquale EB. 2007. Splice variants and expression patterns of SHEP1, BCAR3 and NSP1, a gene family involved in integrin and receptor tyrosine kinase signaling. *Gene* **391**:161-70. doi: 10.1016/j.gene.2006.12.016.

von Wichert G, Jiang G, Kostic A, De Vos K, Sap J, Sheetz MP. 2003. RPTP-alpha acts as a transducer of mechanical force on alphav/beta3-integrin-cytoskeleton linkages. *J Cell Biol* **161**:143-53. doi: 10.1083/jcb.200211061.

Vuori K, Hirai H, Aizawa S, Ruoslahti E. 1996. Induction of p130cas signaling complex formation upon integrin-mediated cell adhesion: a role for Src family kinases. *Mol Cell Biol* **16**:2606-13.

Vuori K, Ruoslahti E. 1995. Tyrosine phosphorylation of p130Cas and cortactin accompanies integrin-mediated cell adhesion to extracellular matrix. *J Biol Chem* **270**:22259-62.

Wallez Y, Mace PD, Pasquale EB, Riedl SJ. 2012. NSP-CAS Protein Complexes: Emerging Signaling Modules in Cancer. *Genes Cancer* **3**:382-93. doi: 10.1177/1947601912460050.

Wallez Y, Riedl SJ, Pasquale EB. 2014. Association of the breast cancer antiestrogen resistance protein 1 (BCAR1) and BCAR3 scaffolding proteins in cell signaling and antiestrogen resistance. *J Biol Chem* **289**:10431-44. doi: 10.1074/jbc.M113.541839.

Webb DJ, Donais K, Whitmore LA, Thomas SM, Turner CE, Parsons JT, Horwitz AF. 2004. FAK-Src signalling through paxillin, ERK and MLCK regulates adhesion disassembly. *Nat Cell Biol* **6**:154-61.

Wilson AL, Schrecengost RS, Guerrero MS, Thomas KS, Bouton AH. 2013. Breast cancer antiestrogen resistance 3 (BCAR3) promotes cell motility by regulating actin cytoskeletal and adhesion remodeling in invasive breast cancer cells. *PLoS One* **8**:e65678. doi: 10.1371/journal.pone.0065678.

Winkelman JD, Anderson CA, Suarez C, Kovar DR, Gardel ML. 2020. Evolutionarily diverse LIM domain-containing proteins bind stressed actin filaments through a conserved mechanism. *Proc Natl Acad Sci U S A* **117**:25532-25542. doi: 10.1073/pnas.2004656117.

Wu X, Suetsugu S, Cooper LA, Takenawa T, Guan JL. 2004. Focal adhesion kinase regulation of N-WASP subcellular localization and function. *J Biol Chem* **279**:9565-76. doi: 10.1074/jbc.M310739200.

Yang X, Boehm JS, Yang X, Salehi-Ashtiani K, Hao T, Shen Y, Lubonja R, Thomas SR, Alkan O, Bhimdi T, Green TM, Johannessen CM, Silver SJ, Nguyen C, Murray RR, Hieronymus H, Balcha D, Fan C, Lin C, Ghamsari L, Vidal M, Hahn WC, Hill DE, Root DE. 2011. A public genome-scale lentiviral expression library of human ORFs. *Nat Methods* **8**:659-61. doi: 10.1038/nmeth.1638.

Yi J, Kloeker S, Jensen CC, Bockholt S, Honda H, Hirai H, Beckerle MC. 2002. Members of the Zyxin family of LIM proteins interact with members of the p130Cas family of signal transducers. *J Biol Chem* **277**:9580-9. doi: 10.1074/jbc.M106922200.

Zadjali F, Pike AC, Vesterlund M, Sun J, Wu C, Li SS, Ronnstrand L, Knapp S, Bullock AN, Flores-Morales A. 2011. Structural basis for c-KIT inhibition by the suppressor of cytokine signaling 6 (SOCS6) ubiquitin ligase. *J Biol Chem* **286**:480-90.

Zaidel-Bar R, Cohen M, Addadi L, Geiger B. 2004. Hierarchical assembly of cell-matrix adhesion complexes. *Biochem Soc Trans* **32**:416-20. doi: 10.1042/BST0320416.

Zaidel-Bar R, Milo R, Kam Z, Geiger B. 2007. A paxillin tyrosine phosphorylation switch regulates the assembly and form of cell-matrix adhesions. *J Cell Sci* **120**:137-48. doi: 10.1242/jcs.03314.

Zhang C, Miller DJ, Guibao CD, Donato DM, Hanks SK, Zheng JJ. 2017. Structural and functional insights into the interaction between the Cas family scaffolding protein p130Cas and the focal adhesion-associated protein paxillin. *J Biol Chem* **292**:18281-18289. doi: 10.1074/jbc.M117.807271.

Zhang W, Lin Y, Liu X, He X, Zhang Y, Fu W, Yang Z, Yang P, Wang J, Hu K, Zhang X, Liu W, Yuan X, Jing H. 2018. Prediction and prognostic significance of BCAR3 expression in patients with multiple myeloma. *J Transl Med* **16**:363. doi: 10.1186/s12967-018-1728-8.

Zhang X, Moore SW, Iskratsch T, Sheetz MP. 2014. N-WASP-directed actin polymerization activates Cas phosphorylation and lamellipodium spreading. *J Cell Sci* **127**:1394-405. doi: 10.1242/jcs.134692.

Zhang Y, Wolf-Yadlin A, Ross PL, Pappin DJ, Rush J, Lauffenburger DA, White FM. 2005. Time-resolved mass spectrometry of tyrosine phosphorylation sites in the epidermal growth factor receptor signaling network reveals dynamic modules. *Mol Cell Proteomics* **4**:1240-50.

Zhang Y, Wolf-Yadlin A, White FM. 2007. Quantitative proteomic analysis of phosphotyrosine-mediated cellular signaling networks. *Methods Mol Biol* **359**:203-12. doi: 10.1007/978-1-59745-255-7_14.

Zhao Z, Tan SH, Machiyama H, Kawauchi K, Araki K, Hirata H, Sawada Y. 2016. Association between tensin 1 and p130Cas at focal adhesions links actin inward flux to cell migration. *Biol Open* **5**:499-506. doi: 10.1242/bio.016428.

Zheng XM, Resnick RJ, Shalloway D. 2000. A phosphotyrosine displacement mechanism for activation of Src by PTPalpha. *Embo J* **19**:964-78.

Figure 1

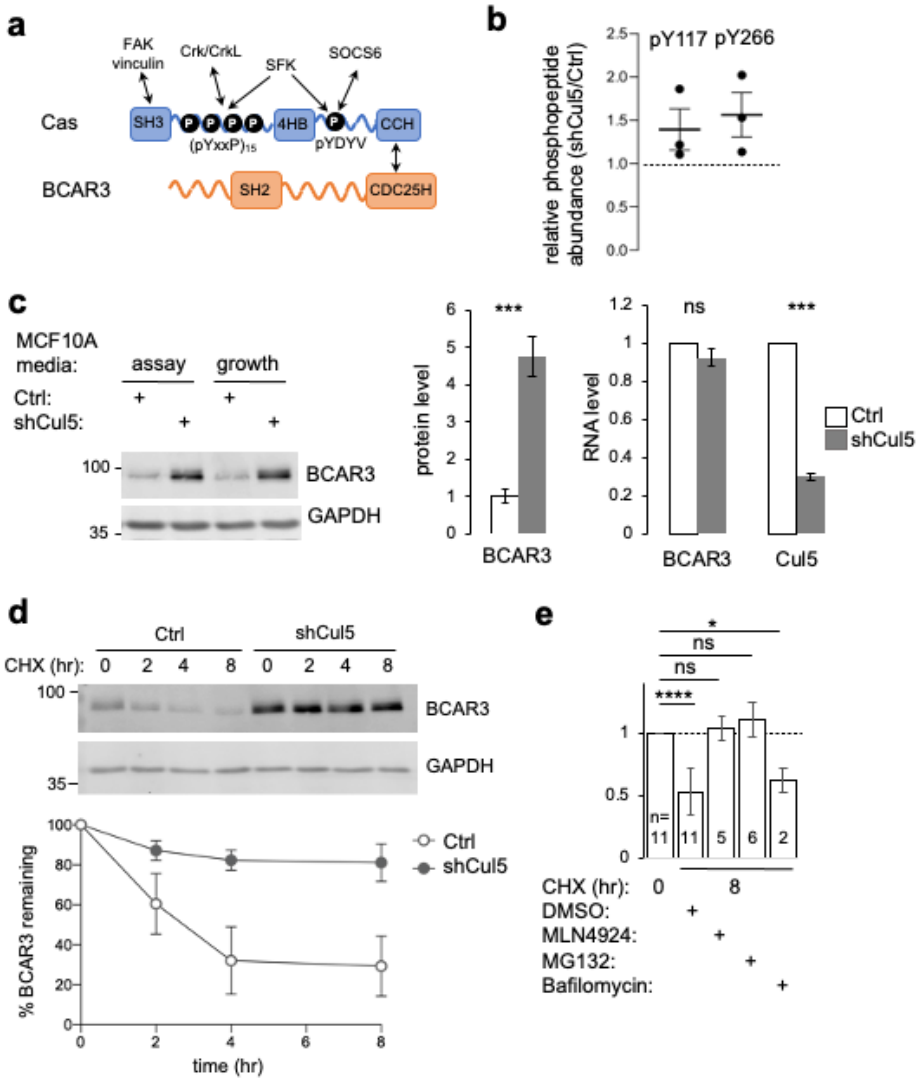

Figure 1. CRL5 regulates BCAR3 protein turnover. (a) Cas and BCAR3 structures. (b) Ratio of BCAR3 pY117 and pY266 phosphopeptide abundances in Cul5-deficient (shCul5) relative to control (Ctrl) MCF10A cells. n=3 biological replicates. (c) BCAR3 protein and RNA levels in Ctrl and shCul5 cells. Representative immunoblot of cells grown in assay media (no added EGF) or growth media (containing EGF). Graphs show immunoblot quantifcation of BCAR3 protein and qPCR quantification of BCAR3 RNA relative to GAPDH control. Mean±SD ; n=3 biological replicates. ***p < 0.001 (t-test). (d) BCAR3 degradation. Control and Cul5-deficient cells were treated with cycloheximide (CHX) for various times. Representative immunoblot and quantification. Mean±SEM ; n=3 biological replicates. (e) Proteasome-dependent BCAR3 degradation. MCF10A cells were treated for 8 hours with CHX and either MLN4924 (cullin neddylation inhibitor), MG132 (proteasome inhibitor) or bafilomycin A1 (lysosome inhibitor). Mean±SD; the number of biological replicates is noted on the graph. *p < 0.05; ****p < 0.0001 (One-way ANOVA).

Figure 1 – figure supplement 1

Protein	Position	Uniprot	Sequence	Experiment 1		Experiment 2	
				Fold[a]	p[b]	Fold[a]	p[b]
KRT6A	Y62	Q92625	sLyGLGGSk	3.21	0.012	1.85	0.011
ABL1	Y393	P00519	lMTGDTyTAHAGAk	2.90	0.010	1.77	0.001
ANKS1A	Y455	Q92625	eEDEHPyELLLTAETk	2.58	0.004	1.41	0.009
ARHGAP35	Y1105	Q9NRY4	nEEENlYsVPHDSTQGk	2.49	0.008	1.67	0.005
RIN1	Y36	Q13671	ekPAQDPLyDVPNASGGQAGGPQRPGR	2.02	0.018	1.45	0.018
BCAR3	Y117	O75815	dPHLLDPTVEyVk	1.96	0.011	1.34	0.049
MPZL1	Y263	O95297	sESVVyADIR	1.90	0.026	1.54	0.027
BCAR3	Y266	O75815	cLEEHyGTSPGQAR	1.81	0.000	1.50	0.012
BCAR1	Y128	P56945	aQQGLyQVPGPSPQFQSPPAk	1.80	0.003	1.28	0.036
SGK223	Y413	Q86YV5	eATQPEPlyAESTk	1.74	0.024	1.26	0.032
ENO1	Y44	P06733	aAVPSGASTGIyEALELR	1.64	0.004	1.18	0.032
ITGB4	Y1207	P16144	vcAYGAQGEGPySSLVScR	1.59	0.010	1.19	0.043
ANXA2	Y30	A6NMY6	ayTNFDAER	1.58	0.018	1.31	0.014
IGF1R	Y1165	P08069	dIYETDyYR	1.53	0.030	1.69	0.001
PTPRA	Y798	P18433	vVQEYIDAFSDyANFk	1.50	0.006	1.23	0.019
TLN1	Y26	Q9Y480	tMQFEPSTMVyDAcR	1.22	0.022	1.25	0.014

Figure 1 – figure supplement 1. Phosphotyrosine peptides increased in Cul5-deficient cells. Protein names, tyrosine positions, Uniprot accession numbers, peptide sequences, and quantification of phosphotyrosine peptides that were significantly increased in two independent experiments, each performed in triplicate, comparing Cul5-deficient and control MCF10A cells. In Experiment 1, the triplicate samples were obtained from cells starved for EGF for 0, 24 or 72 hours. In Experiment 2, the triplicate samples were all from unstarved cells. [a] Ratio shCul5/Ctrl. [b] p value, t-test (2-tailed, paired); n=3.

Figure 2

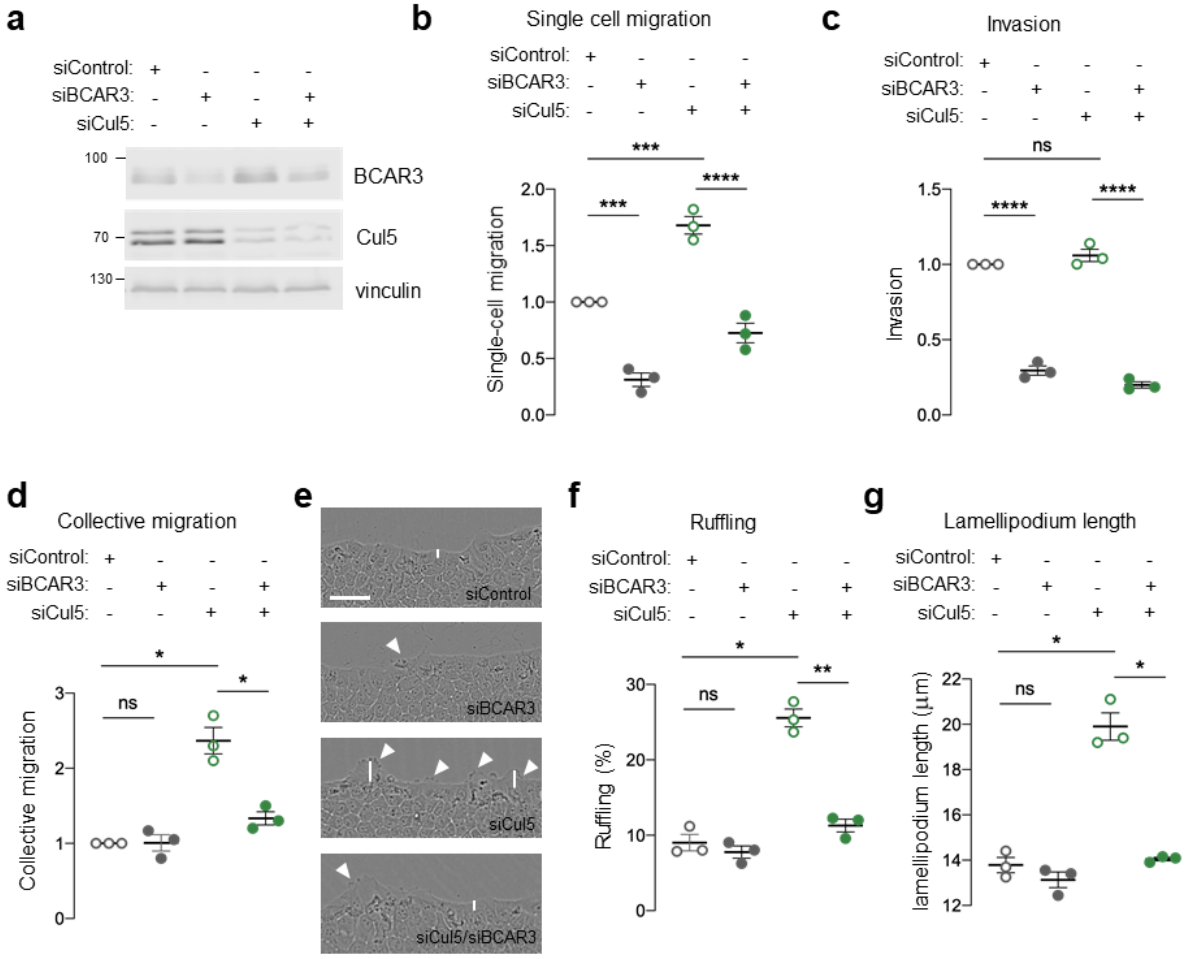

Figure 2. BCAR3 regulates epithelial cell migration. MCF10A cells were transfected with control, BCAR3 or Cul5 siRNA. (a) Representative immunoblot showing BCAR3, Cul5 and vinculin protein levels. (b) Single cell migration using Boyden chamber assay. Migration from EGF-free assay media towards EGF-containing growth media was measured. Mean±SEM; n=3 biological replicates, each with 5 technical replicates. ***p<0.0005 and ****p<0.0001 (One-way ANOVA). (c) Invasion using Boyden chamber containing Matrigel. Mean±SEM; n=3 biological replicates, each with 5 technical replicates. ****p<0.0001 (One-way ANOVA). (d-g) Collective migration. Confluent monolayers were placed in EGF-free media and wounded. (d) Relative migration after 12 hours. Mean±SEM; n=3 biological replicates each with 8-12 technical replicates. *p<0.05 (One-way ANOVA). (e) Representative images of scratch wounds after 6 hours of migration. Arrows indicate cells with membrane ruffles and lines indicate lamellipodia length measurements. Scale bar: 100 µm. (f) Percentage of ruffling cells. Mean±SEM of >250 cells per condition from n=3 biological replicates. *p<0.05 and **p<0.005 (One-way ANOVA). (g) Lamellipodia length. Mean±SEM of 50 cells per condition from n=3 biological replicates. *p<0.05 (One-way ANOVA).

Figure 2 – figure supplement 1

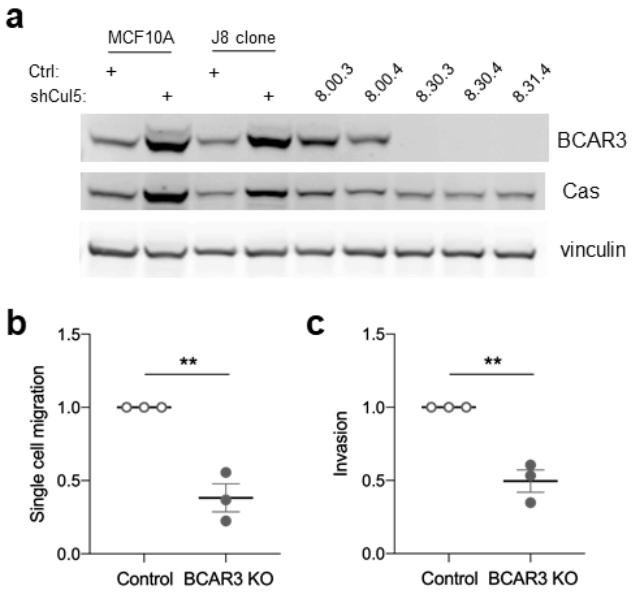

Figure 2 - figure supplement 1. ***BCAR3*** **gene deletion inhibits single-cell migration and invasion**. (a) MCF10A subclone J8, selected for its epithelial morphology, was infected with an all-in-one CRISPR plasmid lacking or containing guide RNA against BCAR3 (guide 30 or 31). Potential knockouts were isolated through single cell expansion. Levels of BCAR3 and Cas in control clonal cell lines, 8.00.3 and 8.00.4, were similar to those in J8 or uncloned MCF10A cells. *BCAR3*-/- (KO) cell lines, 8.30.3, 8.30.4, and 8.31.4, express Cas but not BCAR3. These clones were confirmed by PCR and sequencing (Materials and Methods). (b) Single-cell migration toward EGF using a Boyden chamber assay. Mean±SEM; n=3. **p=0.003 (unpaired t-test). (c) Invasion through Matrigel toward EGF. Mean±SEM; n=3. **p=0.0028 (unpaired t-test).

Figure 3

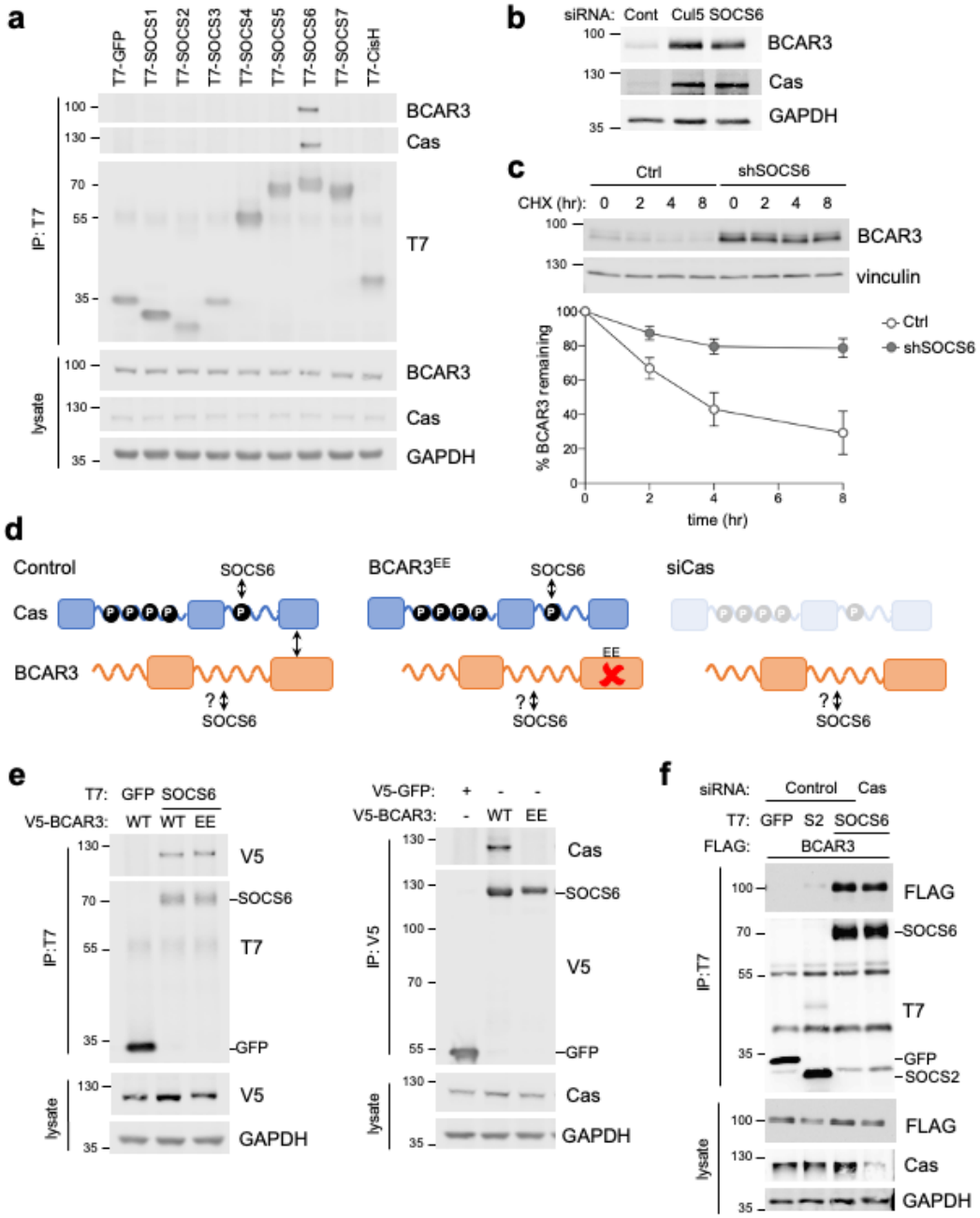

Figure 3. SOCS6 regulates BCAR3 stability independently from Cas. (a) SOCS6 binds BCAR3 and Cas. HeLa cells were transfected with T7-tagged GFP or SOCS proteins and treated with pervanadate for 30 minutes before lysis. Lysates were immunoprecipitated with T7 antibody and immunoprecipitates and lysates were immunoblotted with antibodies to BCAR3, Cas and T7. (b) SOCS6 regulates BCAR3 protein level. MCF10A cells were transfected with control, Cul5 or SOCS6 siRNA and analyzed by immunoblotting. (c) BCAR3 degradation. MCF10A control and SOCS6-deficient cells were treated with cycloheximide (CHX) for various times. Representative immunoblot and quantification. Mean±SEM; n=3 biological replicates. (d) Strategy for testing whether SOCS6 binding to BCAR3 requires Cas. (e) BCAR3 LxxE/RxxE mutation inhibits binding to Cas but not SOCS6. Left panel: HeLa cells were

transfected with control vector or T7-SOCS6 and SNAP-V5-BCAR3^{WT} or SNAP-V5-BCAR3^{EE}. The transfected cells were treated with pervanadate and lysed. Lysates were immunoprecipitated with T7 antibody and immunoprecipitates and lysates were immunoblotted with V5 and T7 antibodies. Right panel: HeLa cells were transfected with control vector, SNAP-V5-BCAR3^{WT} or SNAP-V5-BCAR3^{EE} and lysed. Lysates were immunoprecipitated with V5 antibody and immunoprecipitates and lysates were immunoblotted with Cas and V5 antibodies. (f) SOCS6 binds BCAR3 in Cas-deficient cells. HeLa cells were treated with control or Cas siRNA and transfected with T7-SOCS6 and 3xFLAG-BCAR3. Lysates were immunoprecipitated with T7 antibody and immunoprecipitates and lysates were immunoblotted with FLAG and Cas antibodies.

Figure 4

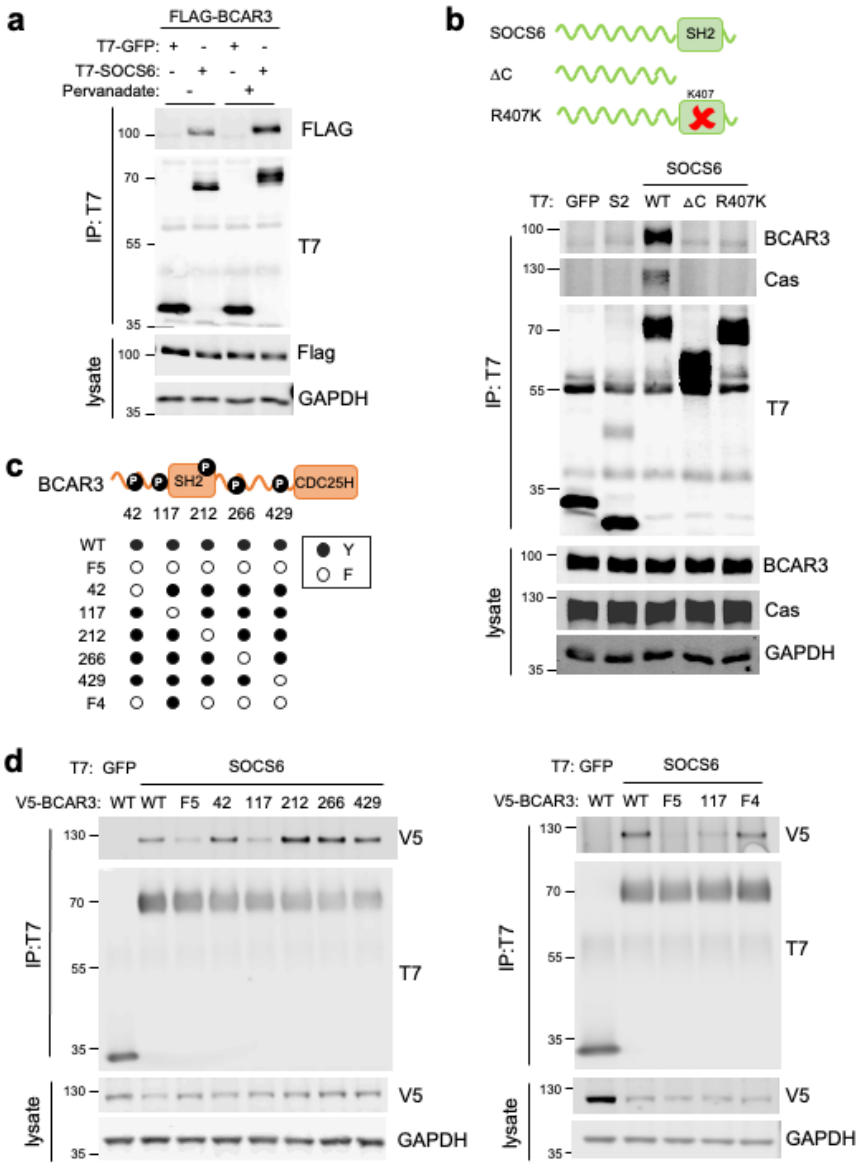

Figure 4. CRL5 binds BCAR3 pY117. (a) Phosphatase inhibition increases SOCS6-BCAR3 binding. HeLa cells were transfected with T7-GFP or T7-SOCS6 and 3xFLAG-BCAR3 and treated with pervanadate or vehicle. Lysates were immunoprecipitated with T7 antibody and immunoprecipitates and lysates were immunoblotted with T7 and FLAG antibodies. (b) SOCS6-BCAR3 binding requires the SOCS6 SH2 domain. Cells were transfected with control vector and T7-tagged SOCS constructs, treated with pervanadate and lysed. Cell lysates were immunoprecipitated with T7 antibody and lysates and immunoprecipitates were immunoblotted with BCAR3 and T7 antibodies. (c) BCAR3^{WT} and phenylalanine (F) mutants. Residues Y42, Y117, Y212, Y266 and Y429 phosphorylation sites have been detected across a range of cell lines (www.PhosphoSite.org). (d) BCAR3 Y117 is necessary and sufficient for SOCS6 binding. HeLa cells were transfected with T7-GFP or T7-SOCS6 and SNAP-V5-BCAR3^{WT} or YF mutants. Transfected cells were treated with pervanadate and lysed. Lysates were immunoprecipitated with T7 antibody and lysates and immunoprecipitates were immunoblotted with V5 and T7 antibodies.

Figure 5

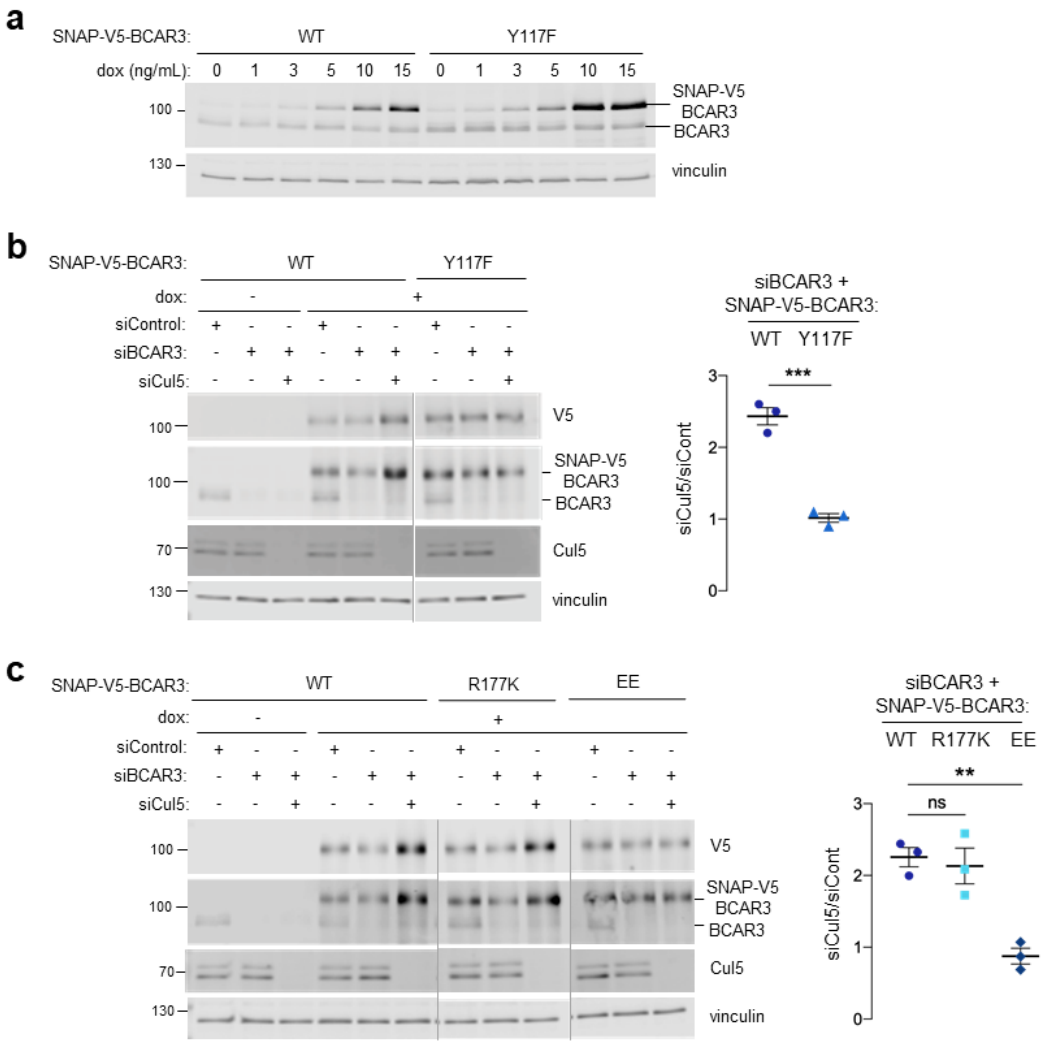

Figure 5. Y117 and Cas regulate BCAR3 protein stability. (a) Y117F mutation increases BCAR3 protein level. SNAP-V5-BCAR3^{WT} and Y117F mutant MCF10A cells were induced with dox concentrations (ng/mL). Lysates were immunoblotted with BCAR3 antibody to detect endogenous and induced SNAP-V5-BCAR3. (b) Cul5 regulates BCAR3 protein level through Y117. Representative immunoblot and quantification of BCAR3 protein in siRNA-treated, dox-induced SNAP-V5-BCAR3^{WT} and Y117F cells. Mean±SEM; n=3 biological replicates. ***p=0.0005 by t-test. (c) Cul5 regulates BCAR3 protein level through Cas binding but not the SH2 domain. As for panel (b), with dox-induced SNAP-V5-BCAR3^{WT}, R177K and EE cells. Vertical lines indicate different immunoblots, each run with its own wildtype control. Mean±SEM; n=3 biological replicates. **p<0.005 by t-test.

Figure 6

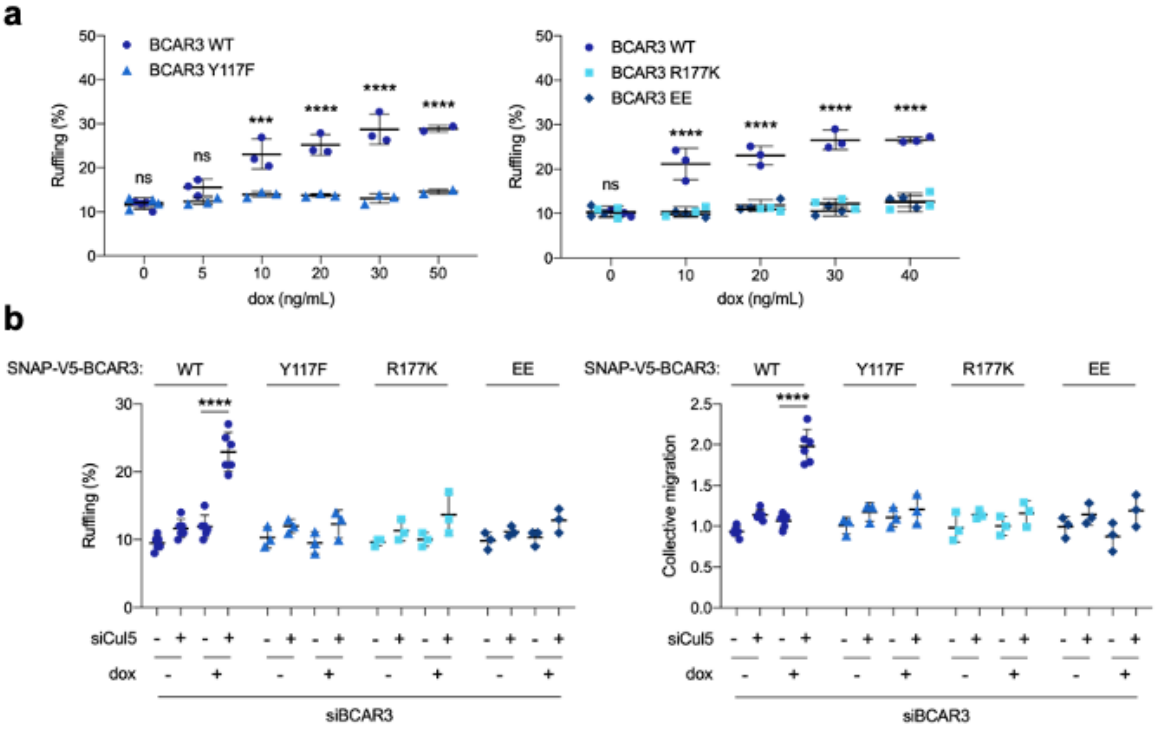

Figure 6. Lamellipodial ruffling and cell migration require multiple BCAR3 domains. (a) Over-expression. SNAP-V5-BCAR3^{WT} and mutant MCF10A cells were induced with various dox concentrations (ng/mL). Confluent monolayers were starved for EGF and wounded. Images of the wounds 6 hours later were used to count the percentage of ruffling cells. Mean±SEM; n=3-6. ***p=0.0001 and ****p<0.0001 (One-way ANOVA). (b) Rescue of ruffling and migration. SNAP-V5-BCAR3^{WT} and mutant MCF10A cells were treated with BCAR3 siRNA and control or Cul5 siRNA and induced with 10 ng/mL dox. Confluent monolayers were placed in EGF-free media and wounded. (Left) Percentage of ruffling cells at 6 hours. Mean±SEM of >250 cells per condition from n=3-6 experiments. ****p<0.0001 (One-way ANOVA). (Right) Relative migration at 12 hours. Mean±SEM; n=3-6 biological replicates, each with 8-12 technical replicates. ****p<0.0001 (One-way ANOVA).

Figure 6 – figure supplement 1

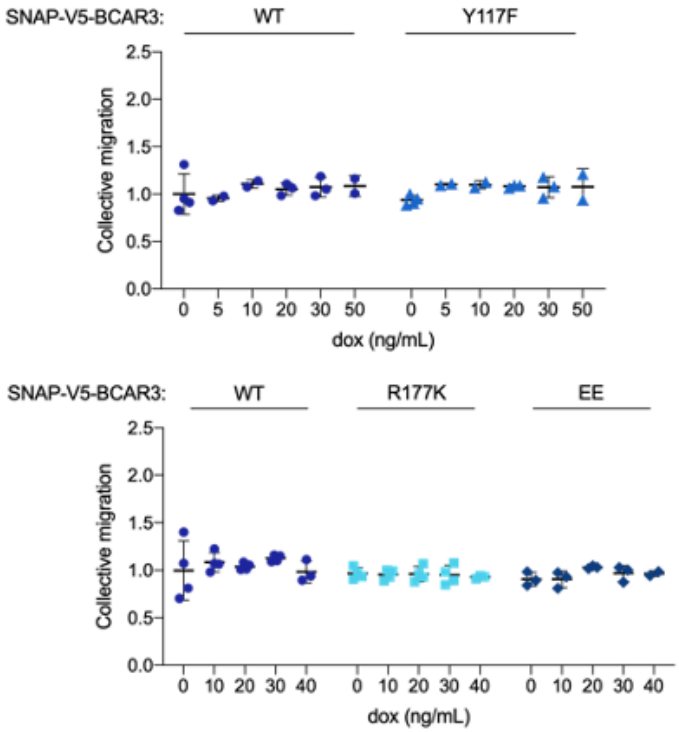

Figure 6 - figure supplement 1. Over-expression of wildtype or mutant BCAR3 does not induce cell migration. SNAP-V5-BCAR3^{WT} and mutant MCF10A cells were induced with various dox concentrations (ng/mL). Confluent monolayers were starved for EGF, scratched and allowed to migrate. Relative migration was measured after 12 hours. Mean±SEM; n=3 biological replicates each with 8-12 technical replicates. $p>0.05$ (One-way ANOVA).

Figure 7

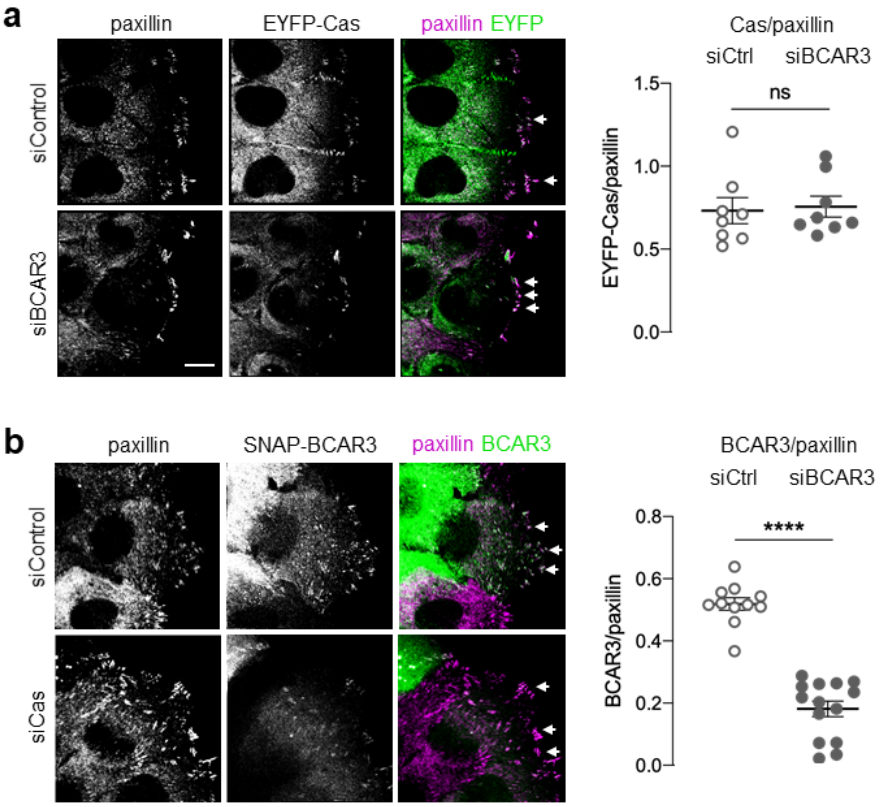

Figure 7. Cas recruits BCAR3 to adhesions. (a) Cas localization does not require BCAR3. MCF10A cells expressing low levels of EYFP-Cas were treated with control or BCAR3 siRNA and allowed to reach confluence. Confluent monolayers were placed in EGF-free media and wounded. After 6 hours, cells were fixed and stained for EYFP-Cas and paxillin. (Left) Maximum intensity projection images. Arrowheads: adhesion sites at the leading edge. Scale bar: 10 µm. (Right) Mean fluorescence intensity of EYFP-Cas relative to paxillin in adhesion sites at the leading edge. Mean±SEM; n=8 cells from 2 biologically independent experiments. p>0.05 by unpaired t-test. (b) BCAR3 localization requires Cas. SNAP-V5-BCAR3^{WT} MCF10A cells were treated with control or Cas siRNA and induced with 10 ng/mL dox. Confluent monolayers were placed in EGF-free media and wounded. After 4 hours, cells were treated with cpJF549-SNAP ligand for one hour. One hour later, they were fixed and stained for paxillin. (Left) Maximum intensity projection images. (Right) Mean fluorescence intensity of SNAP-BCAR3 relative to paxillin in adhesion sites at the leading edge. Mean±SEM; n=11-14 cells from 2 biologically independent experiment. ****p<0.0001 by unpaired t-test.

Figure 8

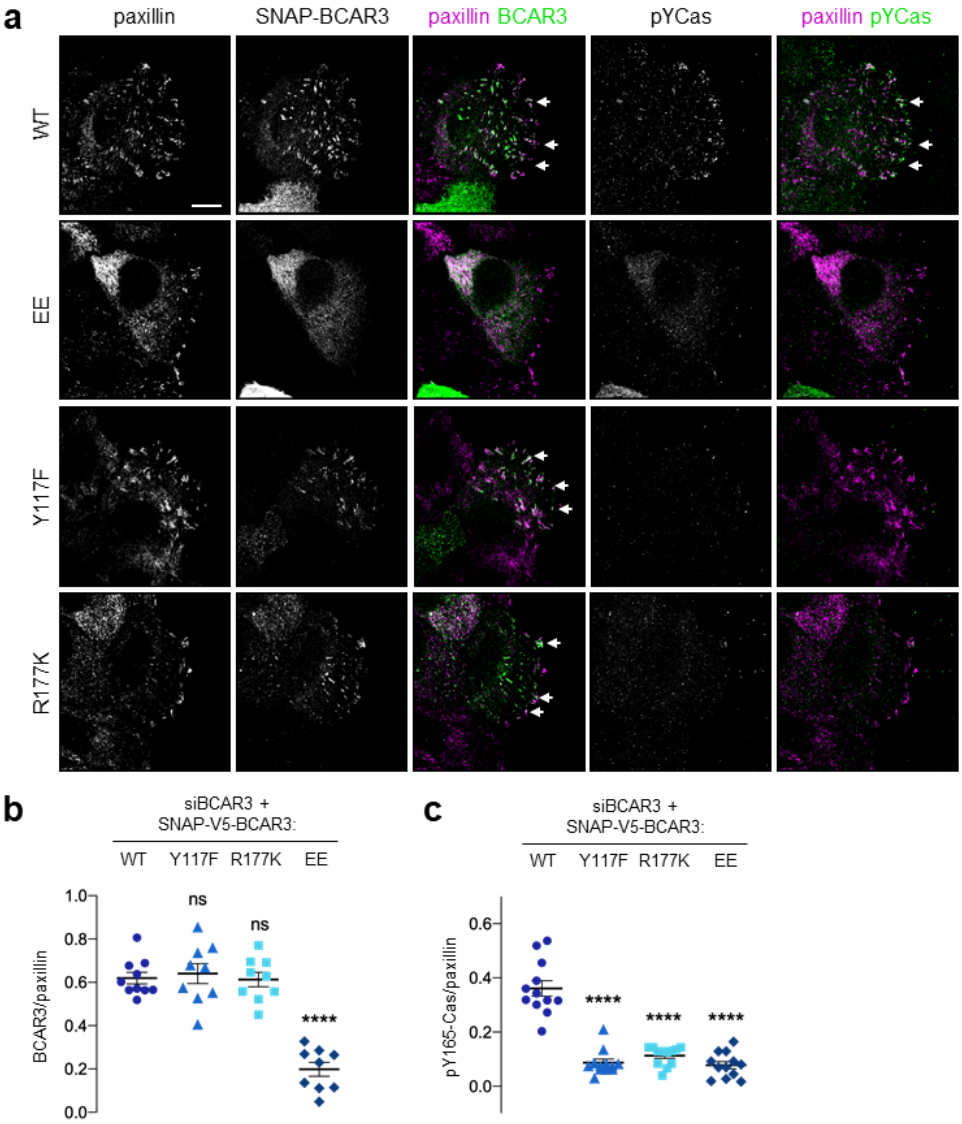

Figure 8. BCAR3 stimulates Cas phosphorylation in adhesions, dependent on BCAR3 Y117 and SH2 interactions. (a) Wildtype or mutant SNAP-V5-BCAR3 MCF10A cells were treated with control or BCAR3 siRNA and induced with 10 ng/mL dox. Confluent monolayers were placed in EGF-free media and wounded. After 4 hours, cells were treated with cpJF549-SNAP ligand for one hour. One hour later, cells were fixed and stained for adhesion marker paxillin and pY165-Cas. Maximum intensity projection. Scale bar = 10 µm. (b) Mean fluorescence intensity of SNAP-V5-BCAR3 relative to paxillin in adhesion sites at the leading edge. Mean±SEM. ****p<0.0001 (One-way ANOVA). (c) Mean fluorescence intensity of pY165-Cas relative to paxillin in adhesion sites at the leading edge. Mean±SEM. ****p<0.0001 (One-way ANOVA).

Figure 8 – figure supplement 1

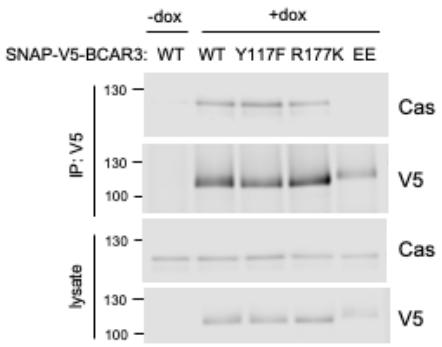

Figure 8 - figure supplement 1. Cas binds to BCAR3 Y117 and SH2 mutants. SNAP-V5-BCAR3^{WT} and mutants were induced in MCF10A cells with 10 ng/mL dox for 48 hours. Lysates were immunoprecipitated with V5 antibody and lysates and immunoprecipitates immunoblotted with Cas and V5 antibodies.

Figure 8 – figure supplement 2

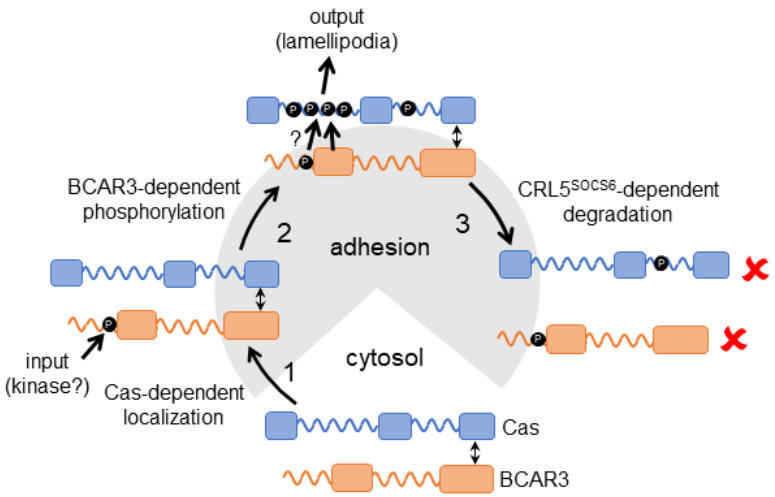

Figure 8 – Figure Supplement 2. Model showing inter-dependence of Cas and BCAR3 for localization and activation. Step 1: A pre-formed BCAR3-Cas complex translocates to integrin adhesions through localization signals in the N and C terminal domains of Cas. Step 2: BCAR3, phosphorylated at Y117 by an unknown kinase, stimulates Cas phosphorylation in a process that also requires the SH2 domain, leading to activation of signaling pathways that stimulate lamellipodial protrusion and ruffling. Step 3: Signaling is terminated by the CRL5SOCS6-dependent ubiquitination and degradation of BCAR3, phosphorylated in their respective phosphodegrons. Remaining questions include the identity of the kinase that phosphorylates BCAR3 Y117, the timing of Y117 phosphorylation, and the mechanism by which BCAR3 pY117 and SH2 domain stimulate Cas phosphorylation.

Figure 8 – figure supplement 3

Protein	Residue	Sequence[a]	Evidence (reference) peptide[b]	mutant[c]	biology[d]
Kit	pY568	gnn**Y**VYIdptq	(1,2)	(1)	
PDGFR	pY579	ghe**Y**IYVdpmq	(2)		
Flt3	pY591	eyf**Y**VdFreye	(3)	(3)	(3)
Flt3	pY919	eei**Y**IiMqscw	(3)	(3)	(3)
Cas	pY664	med**Y**dYVhlqg		(4)	(4)
Dab1	pY198	dpv**Y**qYIvfea		(5)	(5-6)
BCAR3	pY117	tve**Y**VkFsker		(7)	(7)
Spot array[e]		xxx**Y**VYIxxxx IFF MWM WVV	(8)		

Figure 8 – figure supplement 3. Sequence alignment of SOCS6 binding sites.

[a] Local sequence aligned to phosphotyrosine (Y). Capital letters indicate residues at +1 to +3 positions that fit the consensus from the spot array.

[b] Phosphopeptide binds to SH2 domain in vitro

[c] Decreased binding of Y to F mutant protein in cells

[d] Y to F mutant is stabilized or gains function in cells

[e] A library of phosphopeptides randomized at positions +1 to +3 was selected by binding to the SOCS6 SH2 domain. Bound peptides were sequenced. Residues selected at each position are shown in decreasing order of preference.

References: (1) (Bayle et al., 2004) (2) (Zadjali et al., 2011) (3) (Kazi et al., 2012) (4) (Teckchandani et al., 2014) (5) (Feng et al., 2009) (6) (Simo et al., 2013) (7) this work, (8) (Krebs et al., 2002).